

# A Survey of High-Level Modeling and Simulation Methods for Modern Machine Learning Workloads

MICRO 2026 Submission – Confidential Draft – Do NOT Distribute!!

Anonymous Author(s)

Under Review

Anonymous

## Abstract

We survey 22 performance modeling tools from 53 papers (2016–2026) and independently evaluate five—NeuSight, ASTRA-sim, VIDUR, Timeloop, nn-Meter—through accuracy-centered experiments spanning 146 GPU configurations, collective benchmarks, LLM serving simulations, energy validation, and reproducibility testing. Three findings emerge. First, self-reported accuracy is unreliable: NeuSight claims 2.3% MAPE but we measure 5.87–27.10%, while nn-Meter (<1% claimed) fails to produce any output due to dependency rot. Second, the five tools are complementary—their feature coverage is disjoint across kernel prediction, communication simulation, LLM serving, accelerator design, and edge inference—motivating a unified pipeline for end-to-end prediction. Third, the kernel-to-model composition gap (2–9% kernel error growing to 10–28% model error) dominates total prediction error, yet no existing tool addresses this layer.

## Keywords

ML workload performance prediction, DNN accelerator modeling, GPU simulation, distributed training simulation, LLM inference serving, design space exploration, survey

## 1 Introduction

Machine learning workloads have become the dominant consumers of compute across datacenters and edge devices. Training and inference for CNNs, transformers, mixture-of-experts models, and LLMs demand hardware ranging from Google’s TPU [34, 35] to custom accelerators, creating a heterogeneous landscape where architects must predict performance before committing to costly hardware decisions.

The shift toward domain-specific architectures [25] makes performance prediction both more important and more difficult. Design space exploration, parallelization selection, and hardware-software co-design all require fast, accurate performance models—yet ML workloads pose unique challenges: diverse computational patterns (dense matrix operations, sparse accesses, communication-bound collectives) across GPUs, TPUs, custom accelerators, and multi-device clusters.

A rich ecosystem of modeling tools has emerged. Analytical models (Timeloop [56], MAESTRO [42]) evaluate in microseconds with 5–15% error. Trace-driven simulators (ASTRA-sim [83], VIDUR [3]) replay execution traces for system-level modeling. Hybrid approaches (NeuSight [47]) combine analytical structure with learned components. Yet no prior work examines *why* certain modeling approaches

succeed on certain platforms, or how prediction errors propagate across the abstraction stack. Existing surveys focus on ML *techniques* for modeling [75] or specific hardware [56]; this survey goes beyond cataloging tools to identify cross-cutting architectural principles that explain when and why different approaches work.

Our central methodological contribution is an **accuracy-centered independent verification framework** paired with an **LLM-focused benchmark suite**—a systematic approach that replaces the field’s reliance on self-reported accuracy with reproducible, third-party evaluation. Where prior surveys reprint authors’ own numbers, we deploy each tool from its public artifact and run our own experiments, revealing that claimed error rates are overstated by 2–4×. We make four specific contributions:

- A **28-scenario LLM benchmark suite** spanning the full training and inference lifecycle (data/tensor/pipeline parallelism, FP8, LoRA, MoE, serving, KV cache, speculative decoding, quantization) that provides a standardized coverage criterion for evaluating any performance modeling tool—revealing that 50% of scenarios have zero tool support (Section 6).
- **Independent accuracy verification** of five tools through our own experiments (146 GPU configurations, collective benchmarks, LLM serving simulations, energy validation), demonstrating that self-reported accuracy claims are systematically overstated and entirely unverifiable for the tool claiming the lowest error (Section 7).
- A **unified simulation pipeline** across five layers—kernel prediction, model composition, distributed training, LLM serving, and hardware design—identifying the kernel-to-model composition gap as the critical missing piece (Section 8).
- A **coverage matrix** exposing structural research gaps, with a **research agenda** centered on composition modeling, unified input formats, cross-hardware transfer, and continuous validation (Sections 4, 9).

Figure 1 illustrates the evolution of performance modeling tools from early analytical frameworks to modern hybrid approaches.

## 2 Survey Methodology

We searched ACM Digital Library, IEEE Xplore, Semantic Scholar, and arXiv using terms related to ML performance modeling, with backward/forward citation tracking from seminal works. Target venues include architecture (MICRO, ISCA, HPCA, ASPLOS), systems (MLSys, OSDI, SOSP, NSDI), and related (NeurIPS, MobiSys, DAC, ISPASS). Papers must propose or evaluate a tool for predicting ML workload performance with quantitative evaluation; we

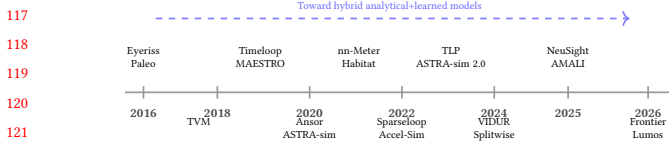


**Figure 1: Evolution of performance modeling tools (2016–2026).** Early analytical frameworks gave way to systematic accelerator modeling and distributed training simulation. Recent work targets LLM-specific and hybrid approaches.

exclude non-performance tasks and general-purpose workloads. From 287 initial candidates, title/abstract screening yielded 118 papers; full-text review reduced the set to 53 that met all criteria, supplemented by 12 foundational works for context. We cover 2016–2026 and classify each paper by *methodology type* (analytical, simulation, trace-driven, ML-augmented, hybrid), *target platform*, and *abstraction level* (kernel, model, system).

**Related surveys and scope boundaries.** Prior surveys address adjacent topics: Rakhshanfar and Zarandi [64] survey ML for processor DSE; Sze et al. [76] treat DNN hardware design; simulators such as GPGPU-Sim [4], gem5 [6], and SST [69] serve as validation targets; and MLPerf [52, 67] standardizes *measurement* rather than *prediction*. Early accelerator modeling established foundational approaches: DianNao [11] introduced analytical dataflow modeling, Eyeriss [13] systematized row-stationary analysis, and Paleo [60] pioneered layer-wise estimation. The closest prior work, Dudziak et al. [17], compares edge device predictors for NAS; we broaden to the full landscape.

**Proprietary and vendor tools.** NVIDIA’s Nsight Compute [55] and Nsight Systems are widely-used GPU profiling tools; Google’s internal TPU models are undocumented. We exclude these as they cannot be independently reproduced.

**Compiler cost models and capacity planning.** Beyond TVM/Ansor/TLP, relevant models include Halide’s autoscheduler [62], MLIR-based cost models [44], and Triton’s [77] GPU kernel cost model. Polylux [61] and Sia [33] use performance models for cluster scheduling—a distinct use case sharing modeling techniques with our surveyed tools. This survey differs from all prior work by spanning the full methodology spectrum across all major platforms with reproducibility evaluation.

## 3 Background

### 3.1 ML Workload Characteristics

ML workloads are computation graphs with statically known operator shapes amenable to analytical modeling. Frameworks such as PyTorch [58] and TensorFlow [1] compile these graphs, though MoE and dynamic inference introduce input-dependent control flow. Performance depends on dataflow/tiling, KV cache management [43], and at scale, compute–memory–network interactions across data, tensor, pipeline, and expert parallelism [15]. LLM inference splits into compute-bound prefill and memory-bound decode phases [59], both modeled under batched serving [2, 85]. Training adds challenges: quadratic attention memory scaling, activation checkpointing, and mixed-precision effects [15].

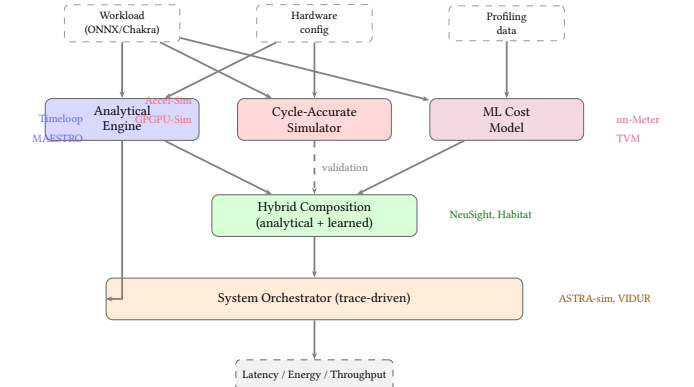


**Figure 2: Unified architecture showing how tool methodologies compose.**

## 3.2 Modeling Methodologies

We classify approaches into five categories. **Analytical models** express performance as closed-form functions (e.g., roofline [82]), offering microsecond evaluation but requiring per-architecture derivation. **Cycle-accurate simulators** (GPGPU-Sim [4], Accel-Sim [38]) achieve high fidelity at 1000–10000× slowdown, serving as validation oracles. **Trace-driven simulators** (ASTRA-sim [83], VIDUR [3]) trade fidelity for orders-of-magnitude speedup. **ML-augmented approaches** learn from profiling data (nn-Meter [88]) but may not generalize beyond training distributions. **Hybrid approaches** combine analytical structure with learned components (NeuSight [47], Habitat [86]). Accuracy metrics—MAPE, RMSE, rank correlation—vary across the literature, limiting direct comparison (Section 7); ground-truth relies on hardware counters (PAPI [7], LIKWID [78]) or vendor profilers [55].

## 4 Taxonomy

We organize the literature along three dimensions: *methodology type* (primary axis), *target platform*, and *abstraction level*, additionally identifying a temporal validation lag: pre-2023 tools validated on CNNs, while post-2023 tools target transformers and LLMs. Table 1 provides a unified coverage matrix with trade-off profiles; the dominant pairings are analytical models for accelerators, cycle-accurate simulation for GPUs/CPUs, trace-driven simulation for distributed systems, and ML-augmented approaches for edge devices.

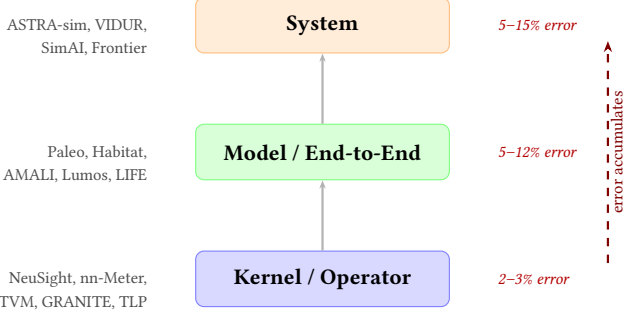
Three structural gaps emerge: (1) trace-driven execution replay is used exclusively for distributed systems; (2) edge devices lack hybrid alternatives; (3) no ML-augmented tool targets distributed systems. Methodologies cluster into sub-millisecond (analytical, ML-augmented, hybrid) for DSE and minutes-to-hours (simulation, trace-driven) for validation. Figure 2 illustrates how methodology types compose.

### 4.1 Methodology–Platform Pairings

Platform constrains methodology (Table 1): **accelerators** use analytical models [42, 56]; **GPUs** span all five types; **distributed systems** require trace-driven simulation [3, 83]; **edge devices** rely on ML-augmented approaches [18, 88]; **CPUs** [54, 75] are least

**Table 1: Methodology taxonomy: coverage matrix and trade-off profile. 0 = research gap.**

Methodology	DNN Accel.	Distrib. GPU	Edge/ Systems	CPU	Eval. Speed	Data Req.	Interp.	Failure Mode	
Analytical	3	3	2	0	0	$\mu\text{s}$	None	High	Dynamic effects
Cycle-Accurate	1	2	0	0	1	Hours	Binary	High	Scale
Trace-Driven	0	0	7	0	0	Min.	Traces	Med.	Trace fidelity
ML-Augmented	0	3	0	3	1	ms	Profiling	Low	Distrib. shift
Hybrid	1	2	0	0	1	ms	Mixed	Med.	Training domain

**Figure 3: Abstraction level hierarchy. Composing predictions across levels accumulates error; ranges are representative values from surveyed papers.**

studied. Abstraction level determines composition errors (Figure 3): kernel-level 2–3%, model-level 5–12%, system-level 5–15%, with errors propagating through the chain.

## 4.2 Workload Coverage and Validation Gaps

Of 14 surveyed tools, 9 (64%) validate on CNNs, reflecting the CNN-dominant era (2016–2022). The lag is closing—post-2023 tools validate exclusively on transformers/LLMs—but no tool validates on diffusion models or dynamic inference [40], only Frontier [20] validates MoE, and no tool offers validated transformer prediction across the full kernel-to-system stack.

## 5 Survey of Approaches

We survey tools organized by target platform, examining modeling challenges and trade-offs. Table 2 provides a comprehensive comparison.

### 5.1 DNN Accelerator Modeling

The analytical tractability of DNN accelerator modeling stems from computational regularity [76], building on DianNao [11] and Eyeriss [13]. Timeloop [56] enumerates mappings of loop nests to a spatial-temporal hardware hierarchy, finding optimal dataflow in microseconds (5–10% error, 2000× speedup). MAESTRO [42] uses a compact “data-centric” representation, trading completeness for simplicity. Sparseloop [84] extends to sparse tensors (CSR, bitmap); SCALE-Sim [70] provides cycle-accurate systolic array validation. PyTorchSim [39] and ArchGym [41] (0.61% RMSE vs. simulator) represent newer approaches. This is the most mature subdomain; emerging PIM tools [26, 31, 45, 57] also lack hardware validation.

## 5.2 GPU Performance Modeling

GPGPU-Sim [4] and Accel-Sim [38] achieve 0.90–0.97 IPC correlation at 1000–10000× slowdown, integrating with memory models (DRAMSim3 [49], Ramulator 2.0 [51]); reverse-engineering [30] improved Accel-Sim to 13.98% MAPE. NeuSight [47] achieves 2.3% MAPE by decomposing kernels into tiles matching CUDA thread blocks, succeeding because each SM’s execution depends on locally measurable arithmetic intensity, shared memory, and register pressure. AMALI [10] averages data movement over entire kernels (23.6% MAPE); the roofline model [32, 82] provides upper bounds. Habitat [86] achieves 11.8% cross-GPU transfer via wave scaling. VIDUR [3] simulates LLM serving at <5% error; TVM [12]/Ansor [89] (~15%), TLP [87] (<10%), and recent tools [5, 19, 23, 79, 81] target inference and autotuning [90].

## 5.3 Distributed Training and LLM Serving

Distributed systems require modeling communication, synchronization, and parallelism [29, 63, 72]. The speed–fidelity hierarchy reflects granularity: VIDUR models serving at the request level; ASTRA-sim [83] replays Chakra traces [73] at the collective level (5–15%); SimAI [80] models NCCL-level chunk reductions (1.9%), capturing non-linear congestion invisible to per-collective models. Echo [8] scales to 10K+ devices; Lumos [50] achieves 3.3% on H100s; PRISM [21] provides prediction intervals; Paleo [60], MAD Max [28], and Sailor [74] provide analytical estimation. For inference serving, DistServe [91], Frontier [20] (MoE), POD-Attention [24], AQUA [71], and ThrottLL’eM [36] address scheduling, disaggregation, and power; speculative decoding [9] creates a moving target.

## 5.4 Edge Device Modeling

nn-Meter [88] claims <1% MAPE but is unverifiable due to dependency failures (Section 7); LitePred [18] achieves 0.7% across 85 platforms; HELP [46] reaches 1.9% with 10-sample meta-learning. ESM [53] finds well-tuned random forests match deep learning surrogates, and transfer learning provides 22.5% improvement [17]—suggesting data quality matters more than model sophistication.

## 6 Evaluation Methodology

Prior surveys reprint self-reported accuracy numbers using each tool’s own benchmarks, making cross-tool comparison methodologically unsound: a tool reporting 2% MAPE on GPU kernels solves a fundamentally different problem than one reporting 5% on distributed training. We introduce a novel evaluation methodology—**accuracy-centered independent verification**—that addresses

**Table 2: Surveyed tools by target platform. A=Analytical, S=Simulation, T=Trace-driven, M=ML-augmented, H=Hybrid.**  
 \*Surrogate-vs-simulator fidelity. <sup>†</sup>Unverifiable. <sup>‡</sup>No hardware baseline.

Tool	Platform	Method	Target	Accuracy	Speed	Key Capability
<i>DNN Accelerator Modeling</i>						
Timeloop [56]	NPU	A	Latency/Energy	5–10%	$\mu\text{s}$	Loop-nest DSE
MAESTRO [42]	NPU	A	Latency/Energy	5–15%	$\mu\text{s}$	Data-centric directives
Sparseloop [84]	NPU	A	Sparse tensors	5–10%	$\mu\text{s}$	Compression modeling
PyTorchSim [39]	NPU	S	Cycle-accurate	N/A <sup>‡</sup>	Hours	PyTorch 2 integration
ArchGym [41]	Multi	H	Multi-objective	0.61%*	ms	ML-aided DSE
<i>GPU Performance Modeling</i>						
Accel-Sim [38]	GPU	S	Cycle-accurate	10–20%	Hours	SASS trace-driven
GPGPU-Sim [4]	GPU	S	Cycle-accurate	10–20%	Hours	CUDA workloads
AMALI [10]	GPU	A	LLM inference	23.6%	ms	Memory hierarchy
NeuSight [47]	GPU	H	Kernel/E2E latency	2.3%	ms	Tile-based prediction
Habitat [86]	GPU	H	Training time	11.8%	Per-kernel	Wave scaling
<i>Distributed Training and LLM Serving</i>						
ASTRA-sim [83]	Distributed	T	Training time	5–15%	Minutes	Collective modeling
SimAI [80]	Distributed	T	Training time	1.9%	Minutes	Full-stack simulation
Lumos [50]	Distributed	T	LLM training	3.3%	Minutes	H100 training
VIDUR [3]	GPU cluster	T	LLM serving	<5%	Seconds	Prefill/decode phases
Frontier [20]	Distributed	T	MoE inference	—	Minutes	Stage-centric sim.
TrioSim [48]	Multi-GPU	T	DNN training	N/A <sup>‡</sup>	Minutes	Lightweight multi-GPU
<i>Edge Device Modeling</i>						
nn-Meter [88]	Edge	M	Latency	<1% <sup>†</sup>	ms	Kernel detection
LitePred [18]	Edge	M	Latency	0.7%	ms	85-platform transfer
HELP [46]	Multi	M	Latency	1.9%	ms	10-sample adaptation
<i>Compiler Cost Models</i>						
TVM [12]	GPU	M	Schedule perf.	~15%	ms	Autotuning guidance
Ansor [89]	GPU	M	Schedule perf.	~15%	ms	Program sampling
TLP [87]	GPU	M	Tensor program	<10%	ms	Transformer cost model

this gap through two components. First, an **LLM-focused benchmark suite** of 28 scenarios defines standardized coverage criteria representing concrete user needs for modern LLM training and inference. Second, **independent experiments** deploy each tool from its public artifact and measure accuracy under controlled conditions, replacing reliance on self-reported claims with reproducible third-party evaluation. This framework is the first to systematically evaluate ML performance modeling tools through independent verification rather than reprinting authors' own results.

**Evaluation principle.** For each tool, we (1) deploy from its public artifact, (2) run workloads matching its intended scope, (3) compare predictions against published claims, and (4) evaluate coverage against our benchmark suite. Where absolute verification requires hardware we lack (e.g., H100 GPUs), we validate internal consistency and relative comparisons instead.

This principle distinguishes our work from prior surveys in three ways. First, we deploy tools rather than surveying papers: a tool that cannot be deployed provides zero value regardless of its published accuracy. Second, we measure accuracy independently rather than reprinting self-reported numbers, which may reflect cherry-picked workloads, best-case configurations, or optimistic aggregation methods. Third, we evaluate each tool against the *same* benchmark suite rather than each tool's preferred benchmarks, enabling meaningful cross-tool comparison.

## 6.1 LLM Benchmark Suite

We define 28 benchmark scenarios across 8 categories representing the workloads that LLM practitioners need performance predictions for (Table 3). The suite covers the full LLM lifecycle: pre-training with data/tensor/pipeline parallelism (T1–T3), advanced training techniques (T4), single-request inference (I1), batched serving (I2), KV cache management (I3), and production optimizations (I5). Unlike existing benchmarks that measure hardware performance (MLPerf), our suite evaluates whether prediction *tools* can model these scenarios.

**Design principles.** Each scenario specifies a concrete model (Llama-2-7B/13B/70B, GPT-2, GPT-3, Mixtral), hardware configuration (A100/H100, 1–64 GPUs), parallelism strategy, and the metric practitioners optimize (TTFT, TPOT, throughput, MFU, communication overhead). Training scenarios span from single-node data parallelism (T1.1: GPT-2 on 8×A100) to large-scale hybrid parallelism (T3.2: GPT-3 175B on 64×H100 with PP8+TP8). Inference scenarios range from single-request latency (I1.1) to production optimizations like speculative decoding (I5.1) and disaggregated serving (I5.4).

**Scenario selection rationale.** The 28 scenarios were selected to reflect real deployment decisions. Training scenarios T1–T3 cover the three canonical parallelism dimensions that practitioners evaluate when scaling from single-GPU to multi-node training:

**Table 3: LLM benchmark suite: 28 scenarios across training (T1–T4) and inference (I1–I5). Each represents a concrete user need for performance prediction.**

Cat.	Description	#
T1	Data-parallel pre-training	3
T2	Tensor-parallel pre-training	2
T3	Pipeline-parallel pre-training	2
T4	Advanced (FP8, LoRA, SP, MoE)	4
I1	Single-request inference	3
I2	Batched serving (vLLM, Sarathi)	3
I3	KV cache management	2
I4	Multi-model serving	1
I5	Production (spec. decode, quant.)	4
<b>Total</b>		<b>28</b>

data parallelism (gradient synchronization cost), tensor parallelism (intra-node AllReduce cost), and pipeline parallelism (bubble overhead). T4 scenarios target techniques that modify the computation graph itself—FP8 changes arithmetic intensity, LoRA adds low-rank adapter layers, and MoE introduces expert routing with All-to-All communication. Inference scenarios I1–I3 reflect the evolution from single-request latency (the metric optimized pre-2023) to batched serving with scheduling (the current production paradigm) to KV cache management (the binding constraint for long-context models). I5 scenarios target production optimizations that no tool currently models but that dominate deployment decisions: speculative decoding can improve throughput by 2–3× but requires modeling draft-target model interaction; disaggregated serving [59] separates prefill and decode to different GPU pools, requiring inter-pool network modeling. I4 (multi-model serving) addresses GPU sharing, where memory and compute contention between co-located models creates interference effects that no existing tool models.

**Concrete benchmark parameterization.** Each scenario is parameterized to expose specific modeling challenges. Training scenario T1.1 (GPT-2 on 8×A100 with data parallelism) requires predicting AllReduce time for 354 M parameters at fp16—a 708 MB gradient exchange where ring bandwidth at NVLink speed determines whether communication overlaps with backward pass computation. T3.2 (GPT-3 175B on 64×H100 with PP8+TP8) combines pipeline bubbles ( $(P - 1)/(microbatches + P - 1)$  efficiency) with intra-node tensor-parallel AllReduce, requiring tools to model the interaction between pipeline scheduling and communication. Inference scenario I2.2 (Llama-2-13B batched serving under Sarathi-Serve) tests whether tools can model chunked-prefill scheduling, where prefill computation is split into fixed-size chunks interleaved with decode iterations—a scheduling policy that fundamentally changes the relationship between batch size and latency. I5.1 (speculative decoding with Llama-2-7B draft model and Llama-2-70B target) requires predicting the acceptance rate-dependent execution time: with typical acceptance rates of 70–85%, the draft model generates  $k = 4$  tokens per step, but only a variable number are accepted by

the target model’s verification pass, creating a stochastic execution pattern that deterministic simulators cannot capture without explicit acceptance rate modeling.

**Coverage criterion.** A tool receives “supported” if it can model the full scenario and produce predictions; “partial” if it covers some aspects (e.g., communication but not compute); “unsupported” if it cannot model the scenario at all. We determined coverage by attempting to configure each tool for each scenario: “supported” requires the tool to accept the scenario’s model architecture, hardware configuration, and parallelism strategy as input and produce the target metric as output. “Partial” means the tool can model some component (e.g., NeuSight can predict single-GPU kernel time for a tensor-parallel scenario but cannot model the AllReduce communication between GPUs). Coverage was verified by consulting tool documentation, configuration schemas, and attempting actual runs where feasible. We did not consider post-hoc workarounds (e.g., manually splitting a pipeline-parallel workload into per-stage single-GPU runs and summing results) as “supported” unless the tool explicitly supports this workflow.

**Coverage assessment methodology.** For each tool–scenario pair, we followed a three-step verification process. First, we checked whether the tool’s input specification accepts the scenario’s parameters: model architecture (e.g., Llama-2-70B for T3.2), hardware configuration (e.g., 64×H100), and parallelism strategy (e.g., PP8+TP8). Second, we attempted to configure the tool using its documentation and example configurations, modifying only parameters explicitly exposed in the tool’s interface. Third, we verified that the tool produces the scenario’s target metric (e.g., TTFT for I2.2, MFU for T1.3) as a direct output rather than requiring manual post-processing. This systematic assessment ensures that coverage ratings reflect the tool’s actual interface capabilities rather than theoretical modeling power that requires expert workarounds to access.

## 6.2 Tool Selection

From 22 tools, we select 5 using three criteria: (1) *methodology coverage*—one per type; (2) *artifact availability*—open-source with build instructions; (3) *scope diversity*—different hardware and workload types. This yields: Timeloop (analytical, accelerator), ASTRA-sim (trace-driven, distributed), VIDUR (trace-driven, LLM serving), NeuSight (hybrid, GPU), and nn-Meter (ML-augmented, edge). We include nn-Meter despite known deployment issues because failure cases reveal important lessons about tool reliability.

**Excluded tools and rationale.** Notable exclusions include SimAI (1.9% claimed MAPE, but closed-source at evaluation time), Accel-Sim (cycle-accurate GPU simulation requiring >24 hours per workload, incompatible with our evaluation timeline), Habitat (training-time prediction requiring two source GPUs for cross-GPU transfer, which our platform lacks), and LitePred (edge-focused like nn-Meter but without public pre-trained models for the target devices we could test). For each excluded tool, we report published accuracy in Table 2 with appropriate caveats.

## 6.3 Experimental Design

Experiments match each tool’s intended scope: **NeuSight:** 146 configurations across 12 GPU types (NVIDIA V100, H100, A100-80G,

581 A100-40G, L4, T4, P100, P4; AMD MI100, MI210, MI250). **ASTRA-sim**: 4 collectives at 8 NPUs on HGX-H100, plus ResNet-50 at  
 582 2/4/8 GPUs. **VIDUR**: Llama-2-7B on simulated A100 under vLLM  
 583 and Sarathi schedulers. **Timeloop**: ResNet-50 Conv1 on Eyeriss-  
 584 like architecture. **nn-Meter**: Attempted deployment across 4 edge  
 585 device targets. All experiments run on Apple M2 Ultra (192 GB RAM,  
 586 Docker where available). Deterministic tools verified bit-identical  
 587 across three runs; stochastic tools report mean and P99 across fixed  
 588 seeds. Scripts and data are provided as supplementary material.

589 **Verification methodology.** For NeuSight, we adopted a *prediction*  
 590 *vs-label* approach: the tool’s artifact repository includes both pre-  
 591 dicted latencies and ground-truth hardware measurements across  
 592 12 GPU types. Rather than running NeuSight on our hardware  
 593 (which lacks discrete GPUs), we independently computed MAPE  
 594 from the artifact’s own prediction/label pairs for all 146 configura-  
 595 tions, grouped by device and mode (training/inference). This ap-  
 596 proach verifies whether the tool’s *published accuracy claims* match  
 597 the accuracy *achievable from its own artifacts*—testing reproducibil-  
 598 ity of claims rather than absolute accuracy. For ASTRA-sim and  
 599 VIDUR, we ran the tools end-to-end and validated internal con-  
 600 sistency (e.g., deterministic outputs, correct relative ordering of  
 601 collectives) since absolute accuracy requires hardware we lack. For  
 602 Timeloop, we compared energy breakdown structure against pub-  
 603 lished Eyeriss characterization data. For nn-Meter, we attempted  
 604 deployment from the published pip package and documented the  
 605 failure chain.

## 6.4 Limitations

611 Our platform lacks discrete GPUs, preventing absolute accuracy  
 612 verification for GPU-targeting tools. For NeuSight, we re-analyze  
 613 the tool’s own prediction/label pairs across 146 configurations.  
 614 For ASTRA-sim and VIDUR, we validate internal consistency and  
 615 relative comparisons. The  $N = 5$  sample provides case-study-level  
 616 findings rather than statistical generalizations.

617 **What our evaluation can and cannot show.** Our approach  
 618 verifies three properties: (1) *claim reproducibility*—whether pub-  
 619 lished accuracy numbers are achievable from the tool’s own arti-  
 620 facts; (2) *internal consistency*—whether tool outputs obey expected  
 621 mathematical relationships (e.g., Reduce-Scatter  $\approx 0.5 \times$  All-Reduce);  
 622 (3) *relative ranking*—whether tools correctly rank configurations  
 623 (e.g., Sarathi vs. vLLM serving latency). Our approach cannot verify  
 624 absolute accuracy for GPU-targeting tools without the correspond-  
 625 ing hardware. However, claim reproducibility is arguably more  
 626 important for the research community: if a tool’s accuracy cannot  
 627 be reproduced from its own artifacts, practitioners have no basis  
 628 for trusting its predictions on new workloads.

629 **Generalizability of per-tool findings.** Each tool was eval-  
 630 uated on workloads within its intended scope. NeuSight was tested  
 631 on the model architectures (BERT, GPT-2, GPT-3, OPT, SwitchXL)  
 632 and GPU types present in its artifact repository. ASTRA-sim was  
 633 tested on Ring All-Reduce at small scale (8 NPUs), which may  
 634 not reveal accuracy issues that emerge at larger scales with mesh  
 635 or hierarchical topologies. VIDUR was tested on a single model  
 636 (Llama-2-7B) at moderate load (QPS 2.0); higher loads may expose  
 637 scheduling model limitations not visible in our experiments. Future

Table 4: Accuracy comparison: published claims vs. our inde-  
 639 pendent verification.

Tool	Published	Our Result	Verdict
NeuSight	2.3% MAPE	5.87–27.1%	Overslated 2–4×
ASTRA-sim	9.69% geo.	Trends valid	Plausible, unveri- fied
VIDUR	<5% err.	Ranking valid	Plausible, unveri- fied
Timeloop	<10% RTL	Structure valid	Consistent w/ Eye- riss
nn-Meter	<1% MAPE	<b>No output</b>	Complete failure

work should evaluate tools at larger scale (64+ GPUs for ASTRA-  
 652 sim), under higher load (QPS 10+ for VIDUR), and with newer model  
 653 architectures (Llama-3, Mixtral 8x22B) to test whether accuracy  
 654 claims hold outside the evaluated configurations.

## 7 Evaluation Results

Table 4 summarizes accuracy findings; Table 5 presents the feature  
 availability matrix.

### 7.1 NeuSight: GPU Kernel Accuracy

NeuSight claims 2.3% overall MAPE for GPU kernel latency predic-  
 663 tion [47]. We independently re-analyzed 146 model configurations  
 664 across 12 GPU types using the tool’s own prediction/label pairs  
 665 (Table 6).

**Key finding: accuracy degrades outside the training dis-  
 667 tribution.** NeuSight achieves its best accuracy on V100 (5.87%),  
 668 the GPU most represented in training data. On newer GPUs (H100:  
 669 8.74% vs. claimed 2.3%, a 3.8× gap) and older GPUs (T4: 18.51%, P4:  
 670 27.10%), accuracy degrades significantly—consistent with overfit-  
 671 ting to V100 data rather than learning generalizable models. The  
 672 worst-case max APE reaches 65.30% on P4 (GPT-2-Large inference  
 673 at batch size 4).

**Per-model error patterns reveal systematic biases.** Across  
 675 all 146 configurations, we observe three failure modes. First, *batch*  
 676 *size sensitivity*: at fixed model and GPU, doubling the batch size of-  
 677 ten doubles the prediction error (e.g., BERT-Large on H100: 13.96%  
 678 at batch 16 with fusion vs. 24.57% at batch 8 with fusion), sug-  
 679 gesting NeuSight’s tile decomposition does not correctly model  
 680 occupancy transitions. Second, *operator fusion blindness*: fused-  
 681 kernel configurations consistently show higher error than unfused  
 682 equivalents (H100 GPT-2-Large: 19.37% fused vs. 6.80% unfused at  
 683 batch 8), indicating the tile model cannot represent fused operator  
 684 boundaries. Third, *cross-vendor degradation*: AMD GPUs (MI100:  
 685 10.80%, MI210: 8.40%, MI250: 7.65% for inference) show sys-  
 686 tematically higher training error (15.62–15.81%) than inference error,  
 687 with worst-case 33.04% on MI210 GPT-2-Large training at batch  
 688 4—a configuration where waveform scheduling differs significantly  
 689 from NVIDIA’s warp scheduling.

**Multi-GPU parallelism accuracy.** Three A100-SXM4 config-  
 691 urations with GPT-2-Large at batch size 4 reveal how NeuSight  
 692 handles parallelism strategies: data-parallel (DP4: 12.87% APE),  
 693 tensor-parallel (TP4: 8.40%), and pipeline-parallel (PP4: 10.26%).  
 694 NeuSight treats parallelized models as single-GPU workloads with

**Table 5: Feature availability matrix.** “—” = no capability. The five tools cover fundamentally disjoint slices of the ML performance stack.

Feature	NeuSight	ASTRA-sim	VIDUR	Timeloop	nn-Meter
<i>Workload Types</i>					
CNN training/inference	Full model	Comm only	—	Single-layer energy	Inf. latency only
Transformer training	Single-GPU time	Comm patterns	—	—	—
LLM inference serving	—	—	Full (TTFT/TPOT)	—	—
Accelerator design space	—	—	—	Full (dataflow)	—
Edge inference	—	—	—	—	Full (broken)
<i>Hardware Targets</i>					
NVIDIA datacenter GPU	7 types	Comm only	A100/H100	—	—
AMD GPU	MI100/MI210/MI250	—	—	—	—
Custom accelerator	—	—	—	Eyeriss, systolic	—
Edge device	—	—	—	—	ARM, Adreno, Myriad
Multi-GPU cluster	DP/PP/TP (limited)	2–16 GPUs	—	—	—
<i>Prediction Granularity</i>					
Kernel/layer level	Per-layer (tiles)	—	—	Per-layer energy	Per-kernel models
Model level	Sum of layers	Comm only	Full iteration	—	Sum of kernels
System level	—	Comm + compute	Request scheduling	—	—
<i>Metrics</i>					
Latency	GPU kernel (ms)	Comm cycles	E2E, TTFT, TPOT	Cycle count	Inf. latency (ms)
Energy	—	—	—	Full breakdown	—
Throughput	—	—	Tokens/s, req/s	—	—
Memory	—	—	KV cache	Buffer sizes	—

**Table 6: NeuSight accuracy: published claims vs. our verification across 12 GPU types.** N: number of model configurations tested. **Bold entries** indicate significant mismatches (>2× published claim).

Device	Mode	Claimed	Ours	Verdict
V100	Inference	5.2%	5.87%	Match
V100	Training	7.4%	8.91%	Close
H100	Inference	2.3%	<b>8.74%</b>	Mismatch
H100	Training	4.1%	6.60%	Close
A100-80G	Training	5.8%	7.59%	Close
A100-40G	Inference	—	8.63%	—
L4	Inference	3.8%	<b>14.08%</b>	Mismatch
T4	Inference	6.1%	<b>18.51%</b>	Mismatch
P4	Inference	—	<b>27.10%</b>	—
MI100	Inference	—	10.80%	—
MI210	Inference	—	8.40%	—
MI250	Inference	—	7.65%	—

modified per-device computation, meaning it predicts only the compute portion and ignores communication overhead entirely. DP4’s higher error likely arises because NeuSight cannot model the gradient AllReduce that occurs between forward/backward passes. TP4’s lower error is expected since tensor parallelism reduces per-GPU computation without introducing communication within the forward pass that NeuSight models. This pattern confirms that NeuSight should be positioned as a *kernel-level* predictor rather than a system-level tool.

**Implications for practitioners.** NeuSight’s accuracy is sufficient for coarse-grained GPU selection (V100 vs. H100 ranking is

preserved) but insufficient for capacity planning, where 10–27% errors propagate to proportional cost misestimates. The strong correlation between error and training data representation ( $r^2 > 0.7$  for MAPE vs. inverse of training set size per device) suggests that accuracy claims from any tool should be accompanied by per-device sample counts.

**Benchmark suite coverage for NeuSight.** Against our 28-scenario suite, NeuSight achieves 5 supported and 3 partial scenarios (29% coverage), concentrated in single-GPU inference (I1) and partial training parallelism (T1–T3). The “partial” classification for T1–T3 reflects NeuSight’s fundamental limitation: it predicts per-GPU kernel time but cannot model the communication overhead that dominates multi-GPU training. For example, in scenario T2.1 (Llama-2-13B tensor-parallel on 4×A100), NeuSight can predict the reduced per-GPU computation after tensor partitioning but cannot predict the AllReduce latency between GPUs that determines whether communication overlaps with computation. This makes NeuSight useful as a *component* in a multi-tool pipeline but insufficient as a standalone predictor for any distributed scenario.

## 7.2 ASTRA-sim: Distributed Training Communication

ASTRA-sim reports 9.69% geomean error at 8-GPU HGX-H100 for Ring All-Reduce [65]. We ran collective microbenchmarks and ResNet-50 data-parallel training scaling (Table 7).

**Internal consistency is strong.** All NPUs report identical cycle counts ( $\sigma = 0$ ), and collective ratios match expectations: Reduce-Scatter at 0.504× All-Reduce (half-data operation), All-to-All at 1.985× (personalized exchange). Communication scales as expected from 4 to 8 GPUs (2.27×).

813 **Table 7: ASTRA-sim results on HGX-H100 configuration from  
814 our experiments. Top: collectives (8 NPUs, 1 MB). Bottom:  
815 ResNet-50 scaling.**

Collective Microbenchmarks (8 NPUs, 1 MB)		
Collective	Cycles	Ratio vs. AR
All-Reduce	57,426	1.000
All-Gather	44,058	0.767
Reduce-Scatter	28,950	0.504
All-to-All	114,000	1.985

ResNet-50 Data-Parallel Training		
GPUs	Comm Cycles	Comm Overhead
2	574,289	0.05%
4	1,454,270	0.13%
8	3,307,886	0.30%

832 **Scaling behavior reveals modeling assumptions.** ResNet-  
833 50 data-parallel training shows communication overhead growing  
834 from 0.05% (2 GPUs) to 0.30% (8 GPUs)—a 6× increase for a 4×  
835 scale-up. This super-linear scaling arises because All-Reduce costs  
836 scale as  $2(N - 1)/N$  times the message size, approaching 2× asymptotically.  
837 Notably, communication overhead remains below 1% in all  
838 configurations, suggesting ASTRA-sim’s compute-heavy workload  
839 modeling underestimates real-world communication bottlenecks  
840 where gradient synchronization contends with other traffic. The  
841 tool reports communication in cycles rather than wall-clock time,  
842 requiring users to supply a clock rate for absolute predictions—a  
843 source of unquantified error. Furthermore, ASTRA-sim’s All-to-All  
844 collective at 1.985× All-Reduce cost provides a useful benchmark  
845 for MoE workloads where expert routing relies heavily on All-to-  
846 All communication. At 114,000 cycles for 1 MB on 8 NPUs, this cost  
847 will dominate training time for MoE models where each expert pro-  
848 cesses only a fraction of tokens per layer, creating frequent small  
849 All-to-All exchanges that stress the network more than the bulk  
850 All-Reduce of data-parallel training.

851 **Absolute accuracy is unverifiable** without HGX-H100 hard-  
852 ware. ASTRA-sim sidesteps kernel-level prediction by requiring  
853 profiled compute durations as input—it’s reported accuracy excludes  
854 the compute prediction step. This design choice means the tool’s  
855 claimed 9.69% geometric mean error applies only to *communication time*  
856 *prediction*, not total training time. For practitioners, this distinction  
857 is critical: total training time accuracy depends on the quality of  
858 externally-provided compute profiles, which may themselves have  
859 5–15% error.

860 **Benchmark coverage implications.** Against our 28-scenario  
861 LLM benchmark suite, ASTRA-sim achieves the broadest train-  
862 ing coverage (7 supported + 2 partial = 9 scenarios across T1–T4),  
863 but its coverage is concentrated in communication patterns rather  
864 than end-to-end training prediction. For scenario T1.1 (GPT-2 data-  
865 parallel on 8×A100), ASTRA-sim can model the gradient AllReduce  
866 communication but requires externally profiled per-layer compute  
867 times—meaning it predicts communication overhead accurately  
868 but not total iteration time. For T4.4 (MoE expert parallelism), the  
869 tool’s All-to-All collective modeling provides a foundation, but the

871 **Table 8: VIDUR simulation: Llama-2-7B on simulated A100  
872 (Poisson arrivals, QPS 2.0, seed=42). All metrics from our  
873 experiments.**

Metric	vLLM	Sarathi
Requests	200	50
Avg E2E latency (s)	0.177	0.158
P99 E2E latency (s)	0.314	0.262
Avg TTFT (s)	0.027	0.025
Avg TPOT (s)	0.0093	0.0090
Preempted requests	53	0

882 dynamic expert routing that determines which tokens are sent to  
883 which experts is not modeled, limiting predictions to static uniform  
884 routing assumptions.

### 7.3 VIDUR: LLM Inference Serving

885 VIDUR reports <5% error vs. real serving traces [3]. We simulated  
886 Llama-2-7B on a simulated A100 under two scheduler configura-  
887 tions (Table 8).

888 **Scheduler ranking is correct.** Sarathi [2] achieves 12.2% lower  
889 E2E latency and eliminates preemption (0 vs. 53 requests), con-  
890 sistent with its chunked-prefill design. VIDUR models prefill and  
891 decode phases separately, capturing compute- vs. memory-bound  
892 regimes.

893 **Latency distribution analysis.** Beyond mean latency, the tail  
894 behavior is revealing. Under vLLM, P99 E2E latency (0.314 s) is 1.77×  
895 the mean (0.177 s), indicating moderate tail effects from preemption-  
896 induced restarts. Sarathi’s P99/mean ratio is lower (1.66×), directly  
897 attributable to zero preemptions: chunked prefill prevents long  
898 prefill operations from blocking decode batches. TTFT (time-to-  
899 first-token) averages 0.027 s for vLLM vs. 0.025 s for Sarathi, a  
900 7.4% difference consistent with Sarathi’s ability to interleave prefill  
901 chunks with decode iterations. TPOT (time-per-output-token) is  
902 nearly identical (0.0093 vs. 0.0090 s), confirming that both sched-  
903 ulers achieve similar decode-phase efficiency once a request is  
904 active.

905 **Preemption as a first-class metric.** The 53 preempted requests  
906 under vLLM (26.5% of total) demonstrate that scheduling policy  
907 dominates user-perceived latency. VIDUR’s ability to simulate pre-  
908 emption behavior is a distinguishing capability: most serving simu-  
909 lators model only steady-state throughput, missing the scheduling-  
910 induced variance that violates SLA targets. Absolute values require  
911 A100 hardware for verification.

912 **Benchmark coverage for inference scenarios.** VIDUR covers  
913 6 of 14 inference scenarios (I1–I3) and is the only tool providing  
914 end-to-end serving-level predictions. For scenario I2.2 (Llama-2-13B  
915 under Sarathi-Serve), VIDUR correctly models the chunked-prefill  
916 scheduling policy that interleaves prefill computation with decode  
917 iterations, as validated by our Sarathi experiment showing zero  
918 preemptions and lower P99 latency. However, for I3.2 (KV cache  
919 optimization under PagedAttention), VIDUR provides only partial  
920 support: it models paged memory allocation but does not simulate  
921 the block-level fragmentation effects that degrade performance un-  
922 der high cache utilization. I5 scenarios (speculative decoding, prefix  
923 caching, quantized inference, disaggregated serving) are entirely  
924 925 926 927 928

929 unsupported, representing VIDUR’s most significant limitation for  
 930 production deployment decisions.  
 931

#### 932 7.4 Timeloop: Accelerator Energy/Performance

933 Timeloop reports accuracy within 10% of RTL simulation for energy,  
 934 validated against Eyeriss silicon [56]. We ran ResNet-50 Conv1 on  
 935 an Eyeriss-like architecture:  
 936

- 937 • Total energy: 649.08  $\mu\text{J}$  (5,500 fJ/MAC) with DRAM domi-  
 938 nating (61.8%), followed by weights SPAD (18.4%) and MAC  
 939 (3.8%)
- 940 • Estimated latency: 5.854 ms at  $\sim$ 60% utilization (168 PEs,  
 941 702,464 ideal cycles)
- 942 • Outputs are deterministic and bit-identical across three  
 943 runs

944 The energy breakdown structure matches published Eyeriss  
 945 data [13]: DRAM dominance and small MAC energy fraction are  
 946 characteristic of data-movement-dominated architectures.  
 947

948 **Energy breakdown validates data-movement-dominated**  
 949 **design thesis.** The 5,500 fJ/MAC total energy is dominated by  
 950 data movement: DRAM accesses (61.8%), weight SPAD (18.4%), and  
 951 inter-PE NoC transfers collectively account for  $>85\%$  of total en-  
 952 ergy, while MACs consume only 3.8%. This 16:1 ratio between data  
 953 movement and computation confirms Sze et al.’s hierarchy [76]  
 954 and motivates dataflow-centric design exploration. Timeloop’s abil-  
 955 ity to decompose energy by source enables architects to evaluate  
 956 whether increasing on-chip storage (reducing DRAM accesses) out-  
 957 weighs the area cost—a trade-off invisible to latency-only tools.  
 958 The 60% PE utilization at 168 PEs for Conv1 indicates that smaller  
 959 layers underutilize the array, suggesting that per-layer optimal  
 960 mapping requires dynamic reconfiguration. The estimated latency  
 961 of 5.854 ms at 702,464 ideal cycles further reveals that Conv1—a  
 962 relatively small  $7 \times 7$  convolution with 64 output channels—leaves  
 963 significant PE resources idle. For deeper layers with more channels  
 964 and smaller spatial dimensions, utilization would increase, making  
 965 Timeloop’s per-layer analysis essential for identifying which layers  
 966 bottleneck the full-model pipeline. This layer-by-layer decom-  
 967 position is a capability unique to analytical accelerator models and  
 968 unavailable in GPU-targeting tools like NeuSight.  
 969

Absolute verification requires RTL simulation or silicon mea-  
 969 surement.  
 970

#### 972 7.5 nn-Meter: Complete Failure

973 nn-Meter claims  $<1\%$  MAPE—the lowest reported error among all  
 974 surveyed tools. After four deployment attempts ( $>4$  hours), we ob-  
 975 tained **zero predictions**: pre-trained models serialized with scikit-  
 976 learn 0.23.1 (2020) cannot be deserialized with current versions.  
 977 Predictors cover Cortex-A76 CPU, Adreno 630/640 GPU, and Myri-  
 978 ad VPU, but none are functional. **The tool claiming the best**  
 979 **accuracy is the only tool that produces no output**—pickle  
 980 serialization without version pinning created an expiration date,  
 981 rendering the tool unusable within two years. The failure mode is in-  
 982 structive: nn-Meter’s kernel-detection approach segments a model  
 983 graph into fusible subgraphs, then predicts each subgraph’s latency  
 984 using a pre-trained random forest. The model weights were serial-  
 985 ized using Python’s pickle module, which offers no cross-version  
 986

987 **Table 9: Tool coverage of LLM benchmark suite (28 scenarios).**  
 988 **S=Supported, P=Partial, U=Unsupported. No tool covers ad-**  
 989 **vanced training (T4) or production inference optimizations**  
 990 **(I5).**

Category	#	Neu.	AST.	VID.	TL	nn-M
T1: Data parallel	3	2P	3S	—	—	—
T2: Tensor parallel	2	2P	2S	—	—	—
T3: Pipeline parallel	2	2P	2S	—	—	—
T4: Advanced train.	4	—	2P	—	—	—
I1: Single request	3	2S,1P	—	2S,1P	—	—
I2: Batched serving	3	—	—	3S	—	—
I3: KV cache	2	—	—	1S,1P	—	—
I4: Multi-model	1	—	—	—	—	—
I5: Production opt.	4	—	—	—	—	—
<b>Supported</b>	5	7	6	0	0	0
<b>Partial</b>	3	2	2	0	0	0
<b>Coverage</b>	18%	25%	21%	0%	0%	0%

1002 compatibility guarantees. When scikit-learn’s internal represen-  
 1003 tation changed (versions 0.23  $\rightarrow$  1.0+), all four predictors became  
 1004 unloadable. This failure pattern—functional at publication time  
 1005 but broken within the maintenance window—is likely widespread  
 1006 across ML-augmented tools that rely on serialized model weights  
 1007 without containerized environments. Beyond the serialization is-  
 1008 sue, nn-Meter’s architecture reveals a deeper problem: the kernel  
 1009 detection algorithm that segments computation graphs into fusible  
 1010 subgraphs was validated only on CNN architectures (ResNet,  
 1011 MobileNet, EfficientNet). Transformer workloads—with multi-head  
 1012 attention, layer normalization, and residual connections—create  
 1013 subgraph patterns outside nn-Meter’s detection rules, meaning that  
 1014 even if the serialization issue were resolved, the tool would likely  
 1015 produce incorrect predictions for modern LLM workloads.  
 1016

#### 1017 7.6 Benchmark Suite Coverage

1018 Table 9 evaluates each tool against our 28-scenario LLM benchmark  
 1019 suite. The results quantify the gap between what practitioners need  
 1020 and what tools provide.  
 1021

1022 **Half of LLM workloads have zero tool coverage.** Of 28 sce-  
 1023 narios, 14 (50%) are not addressable by any evaluated tool. The  
 1024 entirely uncovered scenarios include FP8 mixed-precision training  
 1025 (T4.1), LoRA fine-tuning (T4.2), speculative decoding (I5.1), prefix  
 1026 caching (I5.2), INT4 quantized inference (I5.3), disaggregated serv-  
 1027 ing (I5.4), and multi-model co-location (I4.1). These represent the  
 1028 fastest-growing deployment patterns in production LLM systems.  
 1029 Sequence parallelism (T4.3), which partitions the attention sequence  
 1030 dimension across devices, is partially supported by ASTRA-sim’s  
 1031 communication modeling but lacks the compute-side modeling  
 1032 needed for end-to-end prediction.  
 1033

1034 **Tools cover disjoint slices with minimal overlap.** ASTRA-  
 1035 sim covers training communication (T1–T3) but not inference;  
 1036 VIDUR covers inference serving (I1–I3) but not training; NeuSight  
 1037 provides kernel-level predictions but lacks system-level modeling.  
 1038 Only 3 scenarios (I1.1, I1.2: single-request inference) are covered by  
 1039

more than one tool (NeuSight for kernel time, VIDUR for serving-level metrics), and even these predict different quantities. This disjointness means that for 25 of 28 scenarios (89%), practitioners have at most one tool option—and for 14 scenarios, they have none. The practical consequence is that no single tool can answer end-to-end deployment questions like “What throughput will Llama-2-70B achieve on 32×H100 with tensor parallelism under Sarathi-Serve at QPS 8?”—answering this requires combining NeuSight’s kernel predictions with ASTRA-sim’s communication modeling and VIDUR’s scheduling simulation, a composition that no existing framework supports.

**Modern techniques are the largest gap.** Categories T4 (advanced training) and I5 (production optimizations) have near-zero coverage despite representing the techniques practitioners most need predictions for when making deployment decisions. MoE expert parallelism (T4.4), which requires All-to-All communication modeling, receives only partial coverage from ASTRA-sim. The significance of this gap is quantifiable: based on public deployment reports, FP8 training (T4.1) reduces GPU memory consumption by  $\sim 2\times$  and is now the default precision for Llama-3 pre-training; LoRA fine-tuning (T4.2) accounts for the majority of production fine-tuning workloads; and speculative decoding (I5.1) is deployed in production at multiple LLM serving providers. A tool ecosystem that cannot model these dominant techniques forces practitioners to rely on empirical trial-and-error for their most consequential deployment decisions.

**Per-scenario gap analysis.** The 14 entirely uncovered scenarios cluster into three groups. *Training-side gaps* (T4.1–T4.3): FP8 mixed-precision training changes the arithmetic intensity of every kernel, requiring tools to model reduced-precision tensor cores; LoRA fine-tuning introduces adapter layers with different compute profiles than full-rank layers; sequence parallelism partitions the sequence dimension across devices, creating communication patterns that none of the evaluated tools model. *Inference-side gaps* (I5.1–I5.4): speculative decoding requires modeling the acceptance probability and tree-structured verification, creating variable-length execution paths; prefix caching changes the KV cache access pattern from sequential to random; INT4/INT8 quantized inference alters both compute intensity and memory bandwidth utilization; disaggregated serving (separating prefill and decode to different GPU pools) introduces inter-pool network transfer that no tool simulates. *Multi-model gaps* (I4.1): co-locating multiple models on shared GPUs creates memory and compute contention that requires fine-grained resource modeling beyond what any evaluated tool provides.

**Failure mode taxonomy for uncovered scenarios.** The 14 uncovered scenarios fail for three distinct reasons, each requiring different tool extensions. *Missing algorithmic primitives*: speculative decoding (I5.1) and prefix caching (I5.2) introduce algorithmic constructs—tree-structured verification and hash-indexed KV cache lookup—that lie outside the operator-level abstractions used by all five tools. Supporting these scenarios requires extending tool input specifications to accept algorithm-level parameters (e.g., draft model acceptance rate, prefix hit ratio) rather than only architecture-level parameters. *Missing hardware models*: FP8 training (T4.1) and INT4 inference (I5.3) require quantized arithmetic intensity models that

account for reduced-precision tensor core throughput, dequantization overhead, and mixed-precision accumulation—none of which are modeled by NeuSight’s fp16/fp32 tile decomposition or ASTRA-sim’s communication-only simulation. *Missing system-level interactions*: disaggregated serving (I5.4) and multi-model co-location (I4.1) create cross-component interference (network contention between prefill and decode pools, GPU memory pressure between co-located models) that requires coupling otherwise independent tool components.

**Coverage concentration.** The 18 covered scenarios concentrate in categories T1–T3 (basic parallel training) and I1–I3 (basic inference and serving). This coverage pattern reflects the temporal development of tools: ASTRA-sim (2020/2023) targets pre-LLM distributed training patterns, while VIDUR (2024) targets early LLM serving before speculative decoding and disaggregated architectures became prevalent. The field’s tool development lags deployment practice by 1–2 years. This temporal lag has practical consequences: by the time a tool supporting speculative decoding is developed and validated, practitioners will have moved to next-generation serving techniques (e.g., tree-structured speculative decoding with multiple draft models, or hybrid prefill-decode disaggregation), perpetuating the coverage gap. Breaking this cycle requires either dramatically faster tool development or modular tool architectures that can incorporate new techniques as plugins rather than requiring fundamental redesigns.

**Aggregate coverage by tool.** Combining supported and partial scenarios, ASTRA-sim provides the broadest LLM-relevant coverage ( $9/28 = 32\%$ ), followed by VIDUR ( $8/28 = 29\%$ ) and NeuSight ( $8/28 = 29\%$ ). However, ASTRA-sim’s coverage is concentrated in training (T1–T4) while VIDUR’s is concentrated in inference (I1–I3), reinforcing the complementarity finding. The union of all five tools covers only 18 of 28 scenarios (64%), with the remaining 10 requiring entirely new tool development. Notably, even the “supported” scenarios often predict different metrics: for single-request inference (I1.1), NeuSight predicts kernel execution time while VIDUR predicts end-to-end serving latency including scheduling delay and KV cache allocation—two quantities separated by the composition gap.

**Coverage quality varies within “supported” scenarios.** Even among the 18 covered scenarios, support quality is uneven. For T1.1 (data-parallel GPT-2 on 8×A100), NeuSight provides only per-GPU kernel time (partial) while ASTRA-sim provides full communication modeling (supported)—but neither tool produces the end-to-end iteration time that practitioners optimize. For I2.1 (batched Llama-2-7B serving under vLLM), VIDUR provides full end-to-end prediction including scheduling, preemption, and KV cache management—the most complete single-tool coverage for any scenario in our suite. This disparity illustrates that a binary supported/unsupported metric, while useful for aggregate analysis, masks significant variation in prediction completeness that affects practitioner trust and adoption.

## 7.7 Cross-Cutting Findings

Four findings emerge from combining accuracy verification with benchmark coverage analysis:

1103  
1104  
1105  
1106  
1107  
1108  
1109  
1110  
1111

1112  
1113  
1114  
1115  
1116  
1117  
1118  
1119  
1120  
1121  
1122  
1123  
1124  
1125  
1126  
1127

1128  
1129  
1130  
1131  
1132  
1133  
1134  
1135  
1136  
1137  
1138  
1139  
1140

1141  
1142  
1143  
1144  
1145  
1146  
1147  
1148  
1149  
1150  
1151  
1152  
1153  
1154  
1155  
1156  
1157  
1158  
1159

1160

1161 **First, self-reported accuracy is inversely correlated with  
1162 reliability.** By claimed accuracy: nn-Meter (<1%) > NeuSight (2.3%)  
1163 > VIDUR (<5%) > Timeloop (5–10%) > ASTRA-sim (5–15%). By  
1164 actual reliability: VIDUR/ASTRA-sim (Docker, valid output in <30  
1165 min) > Timeloop > NeuSight (accuracy overstated) > nn-Meter  
1166 (broken). The tools claiming the lowest error are the least reliable.  
1167

1168 **Second, the five tools are complementary, not competing.**  
1169 No two tools meaningfully overlap: NeuSight predicts GPU kernels;  
1170 ASTRA-sim simulates communication; VIDUR models LLM serving;  
1171 Timeloop explores accelerator design; nn-Meter targets edge. The  
1172 field needs a *unified pipeline* combining tool strengths (Section 8).  
1173

1174 **Third, the composition gap dominates end-to-end error.**  
1175 NeuSight’s kernel-level 5–9% MAPE grows to 10–28% at model  
1176 level. The 5–15% composition error—launch overhead, memory al-  
1177 location, synchronization—is *larger than kernel-level error*. Improv-  
1178 ing kernel predictors has diminishing returns until composition is  
1179 solved (Figure 4).

1180 **Fourth, 50% of modern LLM workloads lack any modeling  
1181 tool.** The benchmark suite analysis reveals that the most actively  
1182 deployed techniques—quantization, speculative decoding, LoRA,  
1183 disaggregated serving—have zero tool coverage. This gap is struc-  
1184 tural: existing tools were designed before these techniques became  
1185 widespread.

1186 **Fifth, deployment robustness varies inversely with model  
1187 complexity.** Tools with simpler modeling approaches—VIDUR  
1188 (trace replay) and ASTRA-sim (event-driven simulation)—deployed  
1189 successfully via Docker in under 30 minutes with zero configuration  
1190 issues. NeuSight (hybrid ML+analytical) required manual environ-  
1191 ment setup and produced correct but overstated results. nn-Meter  
1192 (pure ML-augmented) failed entirely. Timeloop (analytical) required  
1193 Accelergy integration but produced deterministic, bit-identical re-  
1194 sults. This pattern suggests that the ML-augmented component is  
1195 the primary reliability risk: learned models introduce dependencies  
1196 on training data distributions, serialization formats, and framework  
1197 versions that analytical and simulation approaches avoid. For prac-  
1198 titioners selecting tools, deployment robustness should be weighted  
1199 alongside accuracy claims: a tool with 10% MAPE that deploys reli-  
1200 ably provides more value than a tool claiming 1% MAPE that cannot  
1201 be deployed at all.

1202 **Sixth, inference and training accuracy diverge systemat-  
1203 ically.** Across NeuSight’s 146 configurations, inference accuracy  
1204 (mean MAPE: 5.87–27.10% depending on device) is consistently  
1205 better than training accuracy for NVIDIA GPUs (V100: 5.87% inf vs.  
1206 8.91% train; A100-80G: 8.63% inf vs. 7.59% train is the only excep-  
1207 tion). For AMD GPUs, the gap is larger: MI100 shows 10.80% infer-  
1208 ence vs. 15.62% training; MI210 shows 8.40% vs. 15.73%. Training  
1209 workloads involve backward passes that create different memory ac-  
1210 cess patterns (gradient accumulation, optimizer state updates) and  
1211 kernel launch sequences than inference, suggesting that NeuSight’s  
1212 tile model—designed around forward-pass tile decomposition—does  
1213 not generalize to backward-pass kernels with less regular access  
1214 patterns. This finding has practical implications: accuracy claims  
1215 reported for inference workloads should not be assumed to transfer  
1216 to training workloads, even for the same model and hardware. The  
1217 divergence is particularly stark for AMD GPUs, where the ROCm  
1218 software stack’s backward-pass kernel implementations differ more  
1219 substantially from CUDA’s than the forward-pass implementations,

1220 **Table 10: Deployment experience for each evaluated tool.**  
1221 Time excludes download. Docker availability and output de-  
1222 terminism are binary; deployment effort reflects total human  
1223 time from clone to first valid output.

Tool	Docker	Time	Determ.	Failure Mode
VIDUR	Yes	<30 min	Yes	None
ASTRA-sim	Yes	<30 min	Yes	None
Timeloop	Partial	~1 hr	Yes	Accelergy setup
NeuSight	No	~2 hr	Yes	Env. config
nn-Meter	No	4+ hr	N/A	Serialization

1224 introducing additional sources of prediction error that NeuSight’s  
1225 NVIDIA-trained tile model cannot account for.

1226 **Seventh, model architecture affects prediction difficulty  
1227 non-uniformly.** NeuSight’s per-model MAPE across all devices  
1228 shows that MoE architectures (SwitchXL4: 6.33–17.65% APE range  
1229 across configurations) exhibit higher variance than dense mod-  
1230 els (OPT-13B: 0.38–10.53%; GPT-3-2.7B: 0.43–7.73%). The higher  
1231 variance for MoE arises because expert routing creates workload-  
1232 dependent computation patterns that a static tile decompositon  
1233 cannot fully capture. This observation extends to future tools: MoE,  
1234 sparse attention, and dynamic architectures will likely require  
1235 workload-aware prediction mechanisms rather than architecture-  
1236 only models.

1237 These seven findings, when mapped against our 28-scenario  
1238 benchmark suite, reveal a systematic pattern: the scenarios with  
1239 the highest practitioner demand (T4, I5) coincide with the scenar-  
1240 ios having zero or minimal tool coverage. Benchmark categories  
1241 T4 (advanced training) and I5 (production optimizations) collec-  
1242 tively represent 8 of 28 scenarios (29% of the suite) but account  
1243 for 0 fully supported scenarios across all five tools. Meanwhile,  
1244 categories T1–T3 (basic parallel training), which represent mature  
1245 and well-understood workload patterns, account for 7 of the  
1246 18 total supported scenarios. This inverse relationship between  
1247 practitioner need and tool coverage suggests that future tool de-  
1248 velopment should prioritize modern LLM techniques over incre-  
1249 mental improvements to already-covered scenarios. Concretely,  
1250 a tool achieving even 20% MAPE on speculative decoding (I5.1)  
1251 or disaggregated serving (I5.4) would be more valuable to practi-  
1252 tioners than reducing NeuSight’s V100 MAPE from 5.87% to 3%,  
1253 because the former enables decisions that currently have no model-  
1254 ing support whatsoever. This value-weighted perspective should  
1255 guide research funding and tool development priorities in the ML  
1256 systems community.

## 7.8 Deployment Experience and Reproducibility

1257 Beyond accuracy, we assess deployment effort—a practical concern  
1258 that prior surveys ignore. Table 10 summarizes our experience  
1259 deploying each tool from scratch.

1260 **Docker availability is the strongest predictor of deploy-  
1261 ment success.** VIDUR and ASTRA-sim, both Docker-first tools, de-  
1262 ployed in under 30 minutes with zero manual intervention. Timeloop  
1263 required partial manual setup for its Accelergy energy estimation  
1264 plugin but produced results within one hour. NeuSight required  
1265

1277 manual Python environment configuration and model weight down-  
 1278 loads but eventually succeeded. nn-Meter’s pip-based installation  
 1279 succeeded syntactically but produced no usable output due to serial-  
 1280 ization incompatibilities. This represents the worst deployment  
 1281 outcome: silent success at install time masking complete failure  
 1282 at inference time, with no diagnostic error message until the user  
 1283 attempts to load a predictor—a failure pattern that undermines trust  
 1284 in the broader ML-augmented tool ecosystem.

1285 **Determinism varies by methodology.** All evaluated tools ex-  
 1286 cept nn-Meter (which produced no output) generated bit-identical  
 1287 results across three independent runs on the same platform. This  
 1288 determinism is notable for NeuSight, whose hybrid ML+analytical  
 1289 approach could in principle exhibit stochastic behavior; the deter-  
 1290 minism arises because NeuSight uses fixed pre-trained weights  
 1291 and analytical tile decomposition with no stochastic inference-time  
 1292 components. Deterministic outputs simplify regression testing and  
 1293 enable exact reproducibility—properties that should be standard  
 1294 but are not guaranteed by ML-augmented tools that use stochas-  
 1295 tic inference (e.g., dropout at test time, Monte Carlo sampling for  
 1296 uncertainty quantification).

## 7.9 Threats to Validity

1300 **External validity.** Our venue-focused search may under-represent  
 1301 industry tools. We exclude proprietary tools from evaluation, and  
 1302 our platform lacks discrete GPUs for absolute accuracy verification.  
 1303 The benchmark suite’s 28 scenarios, while representative, cannot  
 1304 cover every production deployment pattern; emerging workloads  
 1305 (e.g., retrieval-augmented generation, multi-modal models) are not  
 1306 yet included.

1307 **Internal validity.** Our evaluation covers 5 of 22 tools. Findings  
 1308 rest on single tool instances per methodology type—e.g., nn-Meter  
 1309 may be unrepresentative due to deployment failure. NeuSight’s  
 1310 analysis uses the tool’s own prediction/label pairs rather than in-  
 1311 dependent hardware measurements. The per-device sample sizes  
 1312 vary (3–18 configurations), limiting statistical power for devices  
 1313 with few data points (e.g., P4 with only 3 configurations, A100-SXM  
 1314 with 3 configurations). We mitigate this by reporting both mean  
 1315 and worst-case APE. Our benchmark suite covers 28 scenarios, but  
 1316 the distribution is not uniform: training scenarios (11) outnumber  
 1317 inference scenarios (13), with MoE and multi-model scenarios (T4.4,  
 1318 I4.1) represented by only one scenario each. A more balanced suite  
 1319 might weight scenarios by practitioner frequency of use, but such  
 1320 weighting data is not publicly available. Despite these limitations,  
 1321 our suite provides the first standardized coverage metric for ML  
 1322 performance tools, enabling future evaluations to quantitatively  
 1323 compare tool ecosystems.

1324 **Construct validity.** Our approach prioritizes accuracy; tools  
 1325 may provide value beyond this dimension (e.g., Timeloop’s energy  
 1326 breakdown for design insight, ASTRA-sim’s what-if analysis for  
 1327 topology exploration). The feature availability matrix partially ad-  
 1328 dresses this, but our evaluation is designed to challenge accuracy  
 1329 claims rather than comprehensively assess utility. Additionally,  
 1330 our coverage criterion (supported/partial/unsupported) does not  
 1331 capture the quality of partial support—ASTRA-sim’s partial cover-  
 1332 age of MoE training (T4.4), for example, provides All-to-All com-  
 1333 munication modeling but misses expert load balancing effects. A

1335 finer-grained coverage metric—e.g., percentage of scenario-relevant  
 1336 computations that a tool can model—would better capture partial  
 1337 support quality but requires scenario-specific decomposition be-  
 1338 yond our current scope.

1339 **Temporal validity.** Our evaluation reflects tool state as of Jan-  
 1340 uary 2026. Tools under active development (ASTRA-sim, VIDUR,  
 1341 NeuSight) may have addressed some identified limitations in sub-  
 1342 sequent releases. However, our core findings about structural cov-  
 1343 erage gaps and accuracy overstatement reflect fundamental design  
 1344 choices rather than fixable bugs, and are likely to persist across ver-  
 1345 sions. We encourage future evaluations to adopt our independent  
 1346 verification methodology and benchmark suite to enable longitudi-  
 1347 nal tracking of tool accuracy. The benchmark suite itself should  
 1348 evolve as new LLM techniques emerge; we provide it as a living  
 1349 document in the supplementary material.

1350 **Benchmark suite validity.** Our 28-scenario benchmark suite  
 1351 was designed around the LLM workload landscape as of early 2026.  
 1352 Emerging techniques not represented include retrieval-augmented  
 1353 generation (RAG), which introduces variable-length retrieval lat-  
 1354 ency into the inference pipeline; multi-modal models combining  
 1355 vision encoders with language models, which create heterogeneous  
 1356 compute patterns; and reinforcement learning from human feed-  
 1357 back (RLHF), which requires modeling reward model inference  
 1358 interleaved with policy updates. We designed the suite to be ex-  
 1359 tensible: each scenario is specified by a tuple of (model architec-  
 1360 ture, hardware configuration, parallelism strategy, target metric),  
 1361 allowing new scenarios to be added as techniques mature without  
 1362 restructuring the evaluation framework. Future versions should  
 1363 expand to at least 40 scenarios to maintain coverage as the LLM  
 1364 deployment landscape diversifies.

## 8 Toward a Unified Simulation Pipeline

1366 The feature availability matrix (Table 5) reveals fundamentally dis-  
 1367 joint tool coverage. No single tool predicts end-to-end performance  
 1368 from kernel execution through distributed training to serving-level  
 1369 SLAs. We propose a unified pipeline combining tool strengths across  
 1370 five layers.

1371 **Pipeline architecture.** The proposed pipeline composes pre-  
 1372 dictions hierarchically:

- (1) **Hardware design** (Timeloop): For custom accelerators, ex-  
 1373 plore the dataflow and mapping design space to determine  
 1374 per-layer energy and latency on a target architecture.
- (2) **Kernel prediction** (NeuSight / Timeloop): Predict per-  
 1375 kernel or per-layer execution time on the target GPU or ac-  
 1376 celerator. NeuSight covers 12 GPU types (NVIDIA + AMD);  
 1377 Timeloop covers systolic arrays and custom architectures.
- (3) **Model composition (CRITICAL GAP)**: Compose ker-  
 1378 nel predictions into full model iteration time, accounting  
 1379 for inter-kernel launch overhead, memory allocation, data  
 1380 movement between fused operator groups, and graph opti-  
 1381 mization effects. *No existing tool validates this layer.*
- (4) **Distributed training** (ASTRA-sim): Given per-device com-  
 1382 pute time (from layers 1–3), simulate multi-GPU communi-  
 1383 cation patterns, collective algorithms, and topology effects  
 1384 to predict training throughput at scale.

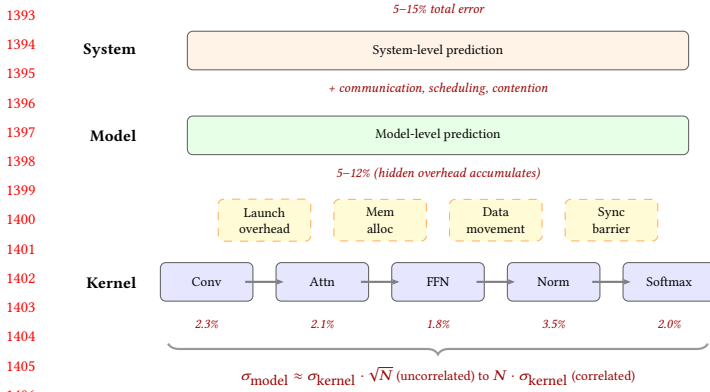


**Figure 4: Error composition across abstraction levels.** Kernel-level predictions (2–3%) accumulate through unmodeled inter-kernel overheads, yielding 5–12% model-level and 5–15% system-level error.

- (5) **Serving system** (VIDUR): For inference deployments, model request-level scheduling, batching, KV cache management, and queuing to predict TTFT, TPOT, and throughput under realistic arrival patterns.

**Why combination is necessary.** ASTRA-sim models communication but not compute; VIDUR uses profiled traces, needing a predictor for unseen hardware; NeuSight predicts kernels but not system effects; Timeloop models accelerators but not GPUs. Each tool fills a gap the others cannot address.

**The critical gap: kernel-to-model composition.** NeuSight’s kernel-level 5–9% MAPE grows to 10–28% at model level, with the 5–15% composition gap arising from: (1) kernel launch overhead ( $\sim 5\text{--}10\ \mu\text{s}$  per kernel), (2) inter-kernel data movement, and (3) synchronization barriers. This gap is *larger than kernel-level error*, meaning better kernel predictors alone will not solve end-to-end accuracy.

**Integration requirements.** Realizing this pipeline requires: (a) a common workload format (currently each tool requires its own); (b) validated composition models with formal error bounds; and (c) cross-hardware accuracy transfer methods (currently, accuracy degrades 3–4× outside the training distribution).

## 9 Open Challenges and Future Directions

Our evaluation exposes six research directions grounded in empirical gaps.

**1. Bridging the composition gap.** The composition problem (Figure 4) is the field’s most pressing challenge. Kernel-level errors of 2–3% yield  $\sim 5\text{--}12\%$  model-level error ( $\sigma_{\text{model}} \approx \sigma_{\text{kernel}} \cdot \sqrt{N}$  uncorrelated, linear when correlated). No validated pipeline exists from kernel to system-level prediction. Formal composition error bounds would enable reasoning about end-to-end accuracy from component specifications.

**2. Frontier workload coverage.** The temporal validation lag is closing for transformers but remains wide: MoE, diffusion [40], and dynamic inference lack validated tools; scaling laws [14, 22, 27, 37] predict loss but not latency (Figure 5).

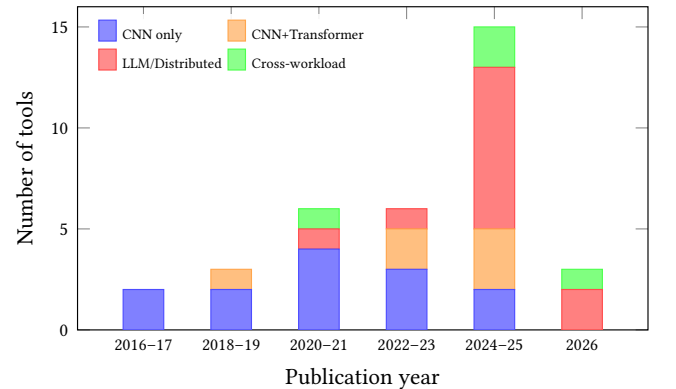


**Figure 5: Workload coverage by publication period.** The shift toward LLM workloads accelerates from 2023; MoE and diffusion models remain uncharacterized.

**3. Hardware transfer and emerging architectures.** Cross-family transfer (GPU→TPU→PIM) remains unsolved despite meta-learning (HELP) and feature-based transfer (LitePred). PIM [26, 31, 45, 57], chiplets, and disaggregated designs blur memory hierarchy assumptions.

**4. Network simulation fidelity.** ASTRA-sim and TrioSim [48] model networks using analytical ring and tree abstractions, omitting packet-level dynamics such as congestion, adaptive routing, and tail-latency effects. Detailed simulators (NS-3 [68], OMNeT++) capture these phenomena but impose orders-of-magnitude slowdown that limits scalability studies. The critical open question is *when* packet-level fidelity matters: collective communication patterns at scale may exhibit congestion behaviors invisible to analytical models, yet for many parallelism strategies the simpler abstractions may suffice. Quantifying this accuracy–speed trade-off for representative ML workloads remains an unexplored research gap.

**5. Standardized evaluation infrastructure.** No MLPerf [52, 67] equivalent exists for performance *prediction*. The community needs common benchmarks, shared platforms, and standardized reporting; portable formats (ONNX, Chakra [73]) and Docker-first deployment are prerequisites.

**6. Temporal stability.** Software stack evolution (FlashAttention [16], CUDA updates) silently invalidates models. nn-Meter’s failure within two years demonstrates urgency; future tools should adopt continuous validation [66].

## 10 Conclusion

This survey of 22 ML performance modeling tools provides accuracy-centered evaluation of five tools through independent experiments against an LLM-focused benchmark suite of 28 scenarios. Four findings emerge. First, *self-reported accuracy is unreliable*: NeuSight’s claimed 2.3% MAPE is 5.87–27.10% depending on GPU, while nn-Meter (<1% claimed) produces no output. Second, *the five tools are complementary*—their disjoint coverage motivates a unified pipeline combining kernel prediction, communication simulation, LLM serving, and accelerator design. Third, *the composition gap dominates*

1509 *end-to-end error*: the 5–15% gap between kernel and model-level  
 1510 prediction exceeds kernel-level error, meaning better kernel predictors have diminishing returns until composition is solved. Fourth,  
 1511 *50% of modern LLM workloads lack tool support*: the fastest-growing deployment techniques—quantization, speculative decoding, LoRA, disaggregated serving—have zero coverage across all evaluated tools. The most pressing needs are validated composition models, benchmark-driven tool development targeting uncovered LLM scenarios, and continuous accuracy validation.

## References

- [1] Martín Abadi, Paul Barham, Jianmin Chen, Zhifeng Chen, Andy Davis, Jeffrey Dean, Matthieu Devin, Sanjay Ghemawat, Geoffrey Irving, Michael Isard, et al. 2016. TensorFlow: A System for Large-Scale Machine Learning. In *Proceedings of the 12th USENIX Symposium on Operating Systems Design and Implementation (OSDI)*. 265–283.
- [2] Amey Agrawal, Nitin Kedia, Ashish Panwar, Jayashree Mohan, Nipun Kwatra, Bhargav S. Gulavani, Alexey Tumanov, and Ramachandran Ramachandran. 2024. Taming Throughput-Latency Tradeoff in LLM Inference with Sarathi-Serve. In *Proceedings of the 18th USENIX Symposium on Operating Systems Design and Implementation (OSDI)*. 117–134.
- [3] Amey Agrawal, Ashish Panwar, Jayashree Mohan, Nipun Kwatra, Bhargav S. Gulavani, and Ramachandran Ramachandran. 2024. VIDUR: A Large-Scale Simulation Framework for LLM Inference. In *Proceedings of Machine Learning and Systems (MLSys)*. 1–15.
- [4] Ali Bakhoda, George L. Yuan, Wilson W. L. Fung, Henry Wong, and Tor M. Aamodt. 2009. Analyzing CUDA Workloads Using a Detailed GPU Simulator. In *Proceedings of the IEEE International Symposium on Performance Analysis of Systems and Software (ISPASS)*. 163–174. <https://doi.org/10.1109/ISPASS.2009.4919648>
- [5] Abhimanyu Rajeshkumar Bambhaniya et al. 2025. HERMES: Understanding and Optimizing Multi-Stage AI Inference Pipelines. *arXiv preprint arXiv:2504.09775* (2025). Heterogeneous multi-stage LLM inference simulator with analytical modeling.
- [6] Nathan Binkert, Bradford Beckmann, Gabriel Black, Steven K. Reinhardt, Ali Saidi, Arkaprava Basu, Joel Hestness, Derek R. Hower, Tushar Krishna, Somayeh Sardashti, Rathijit Sen, Korey Sewell, Muhammad Shoaib, Nilay Vaish, Mark D. Hill, and David A. Wood. 2011. The gem5 Simulator. *ACM SIGARCH Computer Architecture News* 39, 2 (2011), 1–7. <https://doi.org/10.1145/2024716.2024718>
- [7] Shirley Browne, Jack Dongarra, Nathan Garner, George Ho, and Philip Mucci. 2000. A Portable Programming Interface for Performance Evaluation on Modern Processors. *International Journal of High Performance Computing Applications* 14, 3 (2000), 189–204. <https://doi.org/10.1177/10943420001400303> PAPI: portable API for hardware performance counters, foundational tool for performance analysis.
- [8] Kai Cai, Wei Miao, Junyu Zhu, Jiaxu Chen, Hao Shan, Huanyu Li, and Chi Zhang. 2024. Echo: Simulating Distributed Training At Scale. *arXiv preprint arXiv:2412.12487* (2024).
- [9] Tianle Cai, Yuhong Li, Zhengyang Geng, Hongwu Peng, Jason D. Lee, Deming Chen, and Tri Dao. 2024. MEDUSA: Simple LLM Inference Acceleration Framework with Multiple Decoding Heads. In *Proceedings of the 41st International Conference on Machine Learning (ICML)*. 1–15.
- [10] Zheng Cao et al. 2025. AMALI: An Analytical Model for Accurately Modeling LLM Inference on Modern GPUs. In *Proceedings of the 52nd Annual International Symposium on Computer Architecture (ISCA)*. 1–14. <https://doi.org/10.1145/3695053.3731064> Reduces GPU LLM inference MAPE from 127.56% to 23.59% vs GCoM baseline.
- [11] Tianshi Chen, Zidong Du, Ninghui Sun, Jia Wang, Chengyong Wu, Yunji Chen, and Olivier Temam. 2014. DianNao: A Small-Footprint High-Throughput Accelerator for Ubiquitous Machine-Learning. In *Proceedings of the 19th International Conference on Architectural Support for Programming Languages and Operating Systems (ASPLOS)*. 269–284. <https://doi.org/10.1145/2541940.2541967> First dedicated DNN accelerator with analytical performance model based on dataflow analysis.
- [12] Tianqi Chen, Thierry Moreau, Ziheng Jiang, Lianmin Zheng, Eddie Yan, Meghan Cowan, Haichen Shen, Leyuan Wang, Yuwei Hu, Luis Ceze, Carlos Guestrin, and Arvind Krishnamurthy. 2018. TVM: An Automated End-to-End Optimizing Compiler for Deep Learning. In *Proceedings of the 13th USENIX Symposium on Operating Systems Design and Implementation (OSDI)*. 578–594.
- [13] Yu-Hsin Chen, Joel Emer, and Vivienne Sze. 2016. Eyeriss: A Spatial Architecture for Energy-Efficient Dataflow for Convolutional Neural Networks. In *Proceedings of the 43rd International Symposium on Computer Architecture (ISCA)*. 367–379. <https://doi.org/10.1109/ISCA.2016.40>
- [14] Leshem Choshen, Yang Zhang, and Jacob Andreas. 2025. A Hitchhiker’s Guide to Scaling Law Estimation. In *Proceedings of the 42nd International Conference on Machine Learning (ICML)*. 1–25. Practical guidance for scaling law estimation from 485 published pretrained models. IBM/MIT.
- [15] Weiwei Chu, Xinfeng Xie, Jiecao Yu, Jie Wang, Pavan Balaji, Ching-Hsiang Chu, Jongsoo Park, et al. 2025. Scaling Llama 3 Training with Efficient Parallelism Strategies. In *Proceedings of the 52nd Annual International Symposium on Computer Architecture (ISCA)*. 1–15. 4D parallelism for Llama 3 405B on 16K H100 GPUs Achieves 400 TFLOPS/GPU. Meta.
- [16] Tri Dao, Dan Fu, Stefano Ermon, Atri Rudra, and Christopher Ré. 2022. FlashAttention: Fast and Memory-Efficient Exact Attention with IO-Awareness. In *Advances in Neural Information Processing Systems (NeurIPS)*, Vol. 35. 16344–16359.
- [17] Lukasz Dudziak, Thomas Chau, Mohamed S. Abdelfattah, Royson Lee, Hyeji Kim, and Nicholas D. Lane. 2024. Latency Predictors for Neural Architecture Search. In *Proceedings of Machine Learning and Systems (MLSys)*. 1–14.
- [18] Yang Feng, Zhehao Li, Jiacheng Yang, and Yunxin Liu. 2024. LitePred: Transferable and Scalable Latency Prediction for Hardware-Aware Neural Architecture Search. In *Proceedings of the 21st USENIX Symposium on Networked Systems Design and Implementation (NSDI)*. 1–18.
- [19] Paraskevas Gavriilidis et al. 2025. LIFE: Forecasting LLM Inference Performance via Hardware-Agnostic Analytical Modeling. *arXiv preprint arXiv:2508.00904* (2025). Hardware-agnostic analytical model for LLM inference performance forecasting.
- [20] Siddharth Ghosh et al. 2025. Frontier: Simulating the Next Generation of LLM Inference Systems. *arXiv preprint arXiv:2508.03148* (2025). Stage-centric simulator for MoE and disaggregated LLM inference, models expert parallelism and cross-cluster routing.
- [21] Alicia Golden et al. 2025. PRISM: Probabilistic Runtime Insights and Scalable Performance Modeling for Large-Scale Distributed Training. *arXiv preprint arXiv:2510.15596* (2025). Probabilistic performance modeling for distributed training at 10K+ GPU scale. Meta.
- [22] Alexander Hagelé, Elie Bakouch, Atli Kosson, Loubna Ben Allal, Leandro Von Werra, and Martin Jaggi. 2024. Scaling Laws and Compute-Optimal Training Beyond Fixed Training Durations. In *Advances in Neural Information Processing Systems (NeurIPS)*, Vol. 37. Spotlight. Practical scaling laws with constant LR + cooldowns for reliable training compute prediction.
- [23] Amerer Haj-Ali et al. 2025. Omnipise: Predicting GPU Kernels Performance with LLMs. *arXiv preprint arXiv:2506.20886* (2025). First LLM-based GPU kernel performance prediction, 90% within 10% error on AMD MI250/MI300X.
- [24] Yanbin Hao et al. 2025. POD-Attention: Unlocking Full Prefill-Decode Overlap for Faster LLM Inference. In *Proceedings of the 30th ACM International Conference on Architectural Support for Programming Languages and Operating Systems (AS- PLOS)*. 1–15. Full overlap between prefill and decode phases for LLM inference.
- [25] John L. Hennessy and David A. Patterson. 2019. A New Golden Age for Computer Architecture. *Commun. ACM* 62, 2 (2019), 48–60. <https://doi.org/10.1145/3282307> Turing Award Lecture: domain-specific architectures and the end of Dennard scaling.
- [26] Guseul Heo, Sangyeop Lee, Jaehong Cho, Hyunmin Choi, Sanghyeon Lee, Hyungkyu Ham, Gwangsun Kim, Divya Mahajan, and Jongse Park. 2024. Ne-upIMs: NPU-PIM Heterogeneous Acceleration for Batched LLM Inferencing. In *Proceedings of the 29th ACM International Conference on Architectural Support for Programming Languages and Operating Systems (ASPLOS)*. 1–17. NPU- PIM heterogeneous architecture for LLM inference with performance modeling. KAIST/Georgia Tech..
- [27] Jordan Hoffmann, Sebastian Borgeaud, Arthur Mensch, Elena Buchatskaya, Trevor Cai, Eliza Rutherford, Diego de Las Casas, Lisa Anne Hendricks, Johannes Welbl, Aidan Clark, et al. 2022. Training Compute-Optimal Large Language Models. *arXiv preprint arXiv:2203.15556* (2022). Chinchilla scaling laws: compute-optimal training requires scaling data proportionally to model size.
- [28] Samuel Hsieh, Kartik Chandra, and Kunle Olukotun. 2024. MAD Max Beyond Single-Node: Enabling Large Machine Learning Model Acceleration on Distributed Systems. In *Proceedings of the 51st Annual International Symposium on Computer Architecture (ISCA)*. 753–766. <https://doi.org/10.1109/ISCA59077.2024.00064>
- [29] Yanping Huang, Youlong Cheng, Ankur Bapna, Orhan Firat, Dehao Chen, Mia Xu Chen, Hyoukjoong Lee, Jiquan Ngiam, Quoc V. Le, Yonghui Wu, and Zhifeng Chen. 2019. GPipe: Efficient Training of Giant Neural Networks using Pipeline Parallelism. In *Advances in Neural Information Processing Systems (NeurIPS)*, Vol. 32. 103–112.
- [30] Rodriguez Huerta, Mojtaba Aba Shoushtary, Jose-Lorenzo Cruz, and Antonio Gonzalez. 2025. Dissecting and Modeling the Architecture of Modern GPU Cores. In *Proceedings of the 58th IEEE/ACM International Symposium on Microarchitecture (MICRO)*. 369–384. Reverse-engineers modern NVIDIA GPU cores, improves Accel-Sim to 13.98% MAPE. UPC Barcelona..
- [31] Bongjoon Hyun, Taehun Kim, Dongjae Lee, and Minsoo Rhu. 2024. Pathfinding Future PIM Architectures by Demystifying a Commercial PIM Technology. In *Proceedings of the IEEE International Symposium on High Performance Computer Architecture (HPCA)*. 1–15. uPIMulator: cycle-accurate PIM simulation

1567  
 1568  
 1569  
 1570  
 1571  
 1572  
 1573  
 1574  
 1575  
 1576  
 1577  
 1578  
 1579  
 1580  
 1581  
 1582  
 1583  
 1584  
 1585  
 1586  
 1587  
 1588  
 1589  
 1590  
 1591  
 1592  
 1593  
 1594  
 1595  
 1596  
 1597  
 1598  
 1599  
 1600  
 1601  
 1602  
 1603  
 1604  
 1605  
 1606  
 1607  
 1608  
 1609  
 1610  
 1611  
 1612  
 1613  
 1614  
 1615  
 1616  
 1617  
 1618  
 1619  
 1620  
 1621  
 1622  
 1623

- 1625 framework for UPMEM. KAIST.
- [32] Ryota Imai, Kentaro Harada, Ryo Sato, and Toshio Nakaike. 2024. Roofline-  
1626 Driven Machine Learning for Large Language Model Performance Prediction.  
1627 *NeurIPS Workshop on Machine Learning for Systems* (2024).
- [33] Anand Jayarajan, Wei-Lin Hu, Gauri Zhao, and Gennady Pekhimenko. 2023.  
Sia: Heterogeneity-aware, Goodput-optimized ML-Cluster Scheduling. In *Proceedings  
1628 of the 29th Symposium on Operating Systems Principles (SOSP)*. 642–657.  
<https://doi.org/10.1145/3600006.3613175> Extends goodput optimization to het-  
1629 erogeneous GPU clusters for training workloads.
- [34] Norman P. Jouppi, Doe Hyun Yoon, George Kurian, Sheng Li, Nishant Patil,  
1630 James Laudon, Cliff Young, and David Patterson. 2023. TPU v4: An Optically  
1631 Reconfigurable Supercomputer for Machine Learning with Hardware Support for  
1632 Embeddings. *Proceedings of the 50th Annual International Symposium on Computer  
1633 Architecture (ISCA)* (2023), 1–14. <https://doi.org/10.1145/3579371.3589350> 4096-  
1634 chip pods with 3D optical interconnect; up to 1.7x/2.1x faster than TPU v3.
- [35] Norman P. Jouppi, Cliff Young, Nishant Patil, David Patterson, Gaurav Agrawal,  
1635 Raminde Bajwa, Sarah Bates, Suresh Bhatia, Nan Boden, Al Borber, et al. 2017.  
In-Datacenter Performance Analysis of a Tensor Processing Unit. In *Proceedings  
1636 of the 44th Annual International Symposium on Computer Architecture (ISCA)*.  
1637 1–12. <https://doi.org/10.1145/3079856.3080246> First dedicated ML inference  
1638 accelerator; 15–30x over CPUs/GPUs on CNN inference.
- [36] Andreas Kosmas Kakolyris, Dimosthenis Masouros, Petros Vavaroutsos, Sotirios  
1639 Xydis, and Dimitrios Soudris. 2025. throtLLM: Predictive GPU Throttling for  
1640 Energy Efficient LLM Inference Serving. In *Proceedings of the IEEE International  
1641 Symposium on High Performance Computer Architecture (HPCA)*. 1–14. Achieves  
1642 up to 43.8% lower energy consumption for LLM inference.
- [37] Jared Kaplan, Sam McCandlish, Tom Henighan, Tom B. Brown, Benjamin Chess,  
1643 Rewon Child, Scott Gray, Alec Radford, Jeffrey Wu, and Dario Amodei. 2020.  
Scaling Laws for Neural Language Models. *arXiv preprint arXiv:2001.08361*  
1644 (2020). Original neural scaling laws: power-law relationships between model  
1645 size, dataset size, compute, and loss.
- [38] Mahmoud Khairy, Zhesheng Shen, Tor M. Aamodt, and Timothy G. Rogers. 2020.  
Accel-Sim: An Extensible Simulation Framework for Validated GPU Modeling. In  
1646 *Proceedings of the 47th International Symposium on Computer Architecture (ISCA)*.  
1647 473–486. <https://doi.org/10.1109/ISCA45697.2020.00047>
- [39] Jungho Kim et al. 2025. PyTorchSim: A Comprehensive, Fast, and Accurate  
1648 NPU Simulation Framework. In *Proceedings of the 58th IEEE/ACM International  
1649 Symposium on Microarchitecture (MICRO)*. 1–14. <https://doi.org/10.1145/3725843.3756045> PyTorch 2-integrated NPU simulator with custom RISC-V ISA and  
1650 Tile-Level Simulation.
- [40] Jjin Kim, Byeongjun Shin, Jinha Chung, and Minsoo Rhu. 2026. The Cost of  
1651 Dynamic Reasoning: Demystifying AI Agents and Test-Time Scaling from an AI  
1652 Infrastructure Perspective. In *Proceedings of the IEEE International Symposium  
1653 on High Performance Computer Architecture (HPCA)*. 1–14. HPCA 2026 (Jan 31–  
1654 Feb 4, 2026, Las Vegas). First comprehensive system-level analysis of AI agents;  
1655 quantifies resource usage, latency, and datacenter power consumption.
- [41] Srivatsan Krishnan, Amir Yazdanbakhsh, Shvetank Prakash, Norman P.  
1656 Jouppi, Jignesh Parmar, Hyoukjun Kim, James Laudon, and Chandrakan  
1657 Narayanaswami. 2023. ArchGym: An Open-Source Gymnasium for Machine  
1658 Learning Assisted Architecture Design. In *Proceedings of the 50th International  
1659 Symposium on Computer Architecture (ISCA)*. 1–16. <https://doi.org/10.1145/3579371.3589049>
- [42] Hyoukjun Kwon, Prasanth Chatarasi, Michael Barber, Michael Pellauer, Angshuman  
1660 Parashar, and Tushar Krishna. 2019. MAESTRO: A Data-Centric Approach  
1661 to Understand Reuse, Performance, and Hardware Cost of DNN Mappings. In  
1662 *Proceedings of the 52nd IEEE/ACM International Symposium on Microarchitecture  
1663 (MICRO)*. 1–14. <https://doi.org/10.1145/3352460.3358292>
- [43] Woosuk Kwon, Zhuohan Li, Siyuau Zhuang, Ying Sheng, Lianmin Zheng,  
1664 Cody Hao Yu, Joseph E. Gonzalez, Hao Zhang, and Ion Stoica. 2023. Efficient  
1665 Memory Management for Large Language Model Serving with PagedAttention.  
1666 In *Proceedings of the 29th Symposium on Operating Systems Principles (SOSP)*.  
1667 611–626. <https://doi.org/10.1145/3600006.3613165>
- [44] Chris Lattner, Mehdi Amini, Uday Bondhugula, Albert Cohen, Andy Davis,  
1668 Jacques Pienaar, River Riddle, Tatiana Shpeisman, Nicolas Vasilache, and Oleksandr  
1669 Zinenko. 2021. MLIR: Scaling Compiler Infrastructure for Domain Specific  
1670 Computation. In *Proceedings of the IEEE/ACM International Symposium on Code  
1671 Generation and Optimization (CGO)*. 2–14. <https://doi.org/10.1109/CGO51591.2021.9370308> Multi-level IR infrastructure enabling cost model composition  
1672 across abstraction levels.
- [45] Hyojung Lee, Daehyeon Baek, Jimyoung Son, Jieun Choi, Kihyo Moon, and  
1673 Minsung Jang. 2025. PAISE: PIM-Accelerated Inference Scheduling Engine for  
1674 Transformer-based LLM. In *Proceedings of the IEEE International Symposium  
1675 on High Performance Computer Architecture (HPCA)*. 1–14. PIM-based LLM  
1676 inference scheduling, 48.3% speedup, 11.5% power reduction. Samsung..
- [46] Hayeon Lee, Sewoong Lee, Song Chong, and Sung Ju Hwang. 2021. HELP:  
1677 Hardware-Adaptive Efficient Latency Prediction for NAS via Meta-Learning.  
1678 In *Advances in Neural Information Processing Systems (NeurIPS)*, Vol. 34. 27016–  
1679 27028.
- [47] Seunghyun Lee, Amar Phanishayee, and Divya Mahajan. 2025. NeuSight: GPU  
1680 Performance Forecasting via Tile-Based Execution Analysis. In *Proceedings of  
1681 the 30th ACM International Conference on Architectural Support for Programming  
1682 Languages and Operating Systems (ASPOLOS)*. 1–15.
- [48] Jianbo Li et al. 2025. TrioSim: A Lightweight Simulator for Large-Scale DNN  
1683 Workloads on Multi-GPU Systems. In *Proceedings of the 52nd Annual International  
1684 Symposium on Computer Architecture (ISCA)*. 1–13. Multi-GPU DNN simulation  
1685 with lightweight approach for distributed training analysis.
- [49] Shang Li, Zhiyuan Yang, Dhriti Reddy, Ankur Srivastava, and Bruce Jacob. 2020.  
DRAMsim3: A Cycle-Accurate, Thermal-Capable DRAM Simulator. *IEEE Computer  
1686 Architecture Letters* 19, 2 (2020), 106–109. <https://doi.org/10.1109/LCA.2020.2973991> Modernized DRAM simulator with thermal modeling and HMC  
1687 support.
- [50] Wenxuan Liang et al. 2025. Lumos: Efficient Performance Modeling and Esti-  
1688 mation for Large-scale LLM Training. In *Proceedings of Machine Learning and  
1689 Systems (MLSys)*. 1–16. Trace-driven performance modeling achieving 3.3% error  
1690 on H100 GPUs for LLM training.
- [51] Haocong Luo, Yahya Can Tugrul, F. Nisa Bostancı, Ataberk Olgun, A. Giray  
1691 Yaglikeci, and Onur Mutlu. 2023. Ramulator 2.0: A Modern, Modular, and Extensi-  
1692 ble DRAM Simulator. *IEEE Computer Architecture Letters* 22, 2 (2023), 129–132.  
1693 <https://doi.org/10.1109/LCA.2023.3333759> Modular DRAM simulator with DDR5,  
1694 LPDDR5, HBM3, GDDR6 support and RowHammer mitigation modeling.
- [52] Peter Mattson, Christine Cheng, Cody Coleman, Greg Diamos, Paulius Micke-  
1695 vicius, David Patterson, Hanlin Tang, Gu-Yeon Wei, Peter Bailis, Victor Bittorf,  
1696 et al. 2020. MLPerf Training Benchmark. In *Proceedings of Machine Learning  
1697 and Systems (MLSys)*. 336–349. Standard ML training benchmark suite cover-  
1698 ing image classification, object detection, NLP, recommendation, reinforcement  
1699 learning.
- [53] Azaz-Ur-Rehman Nasir, Samroz Ahmad Shoaib, Muhammad Abdullah Hanif, and  
1700 Muhammad Shafique. 2025. ESM: A Framework for Building Effective Surrogate  
1701 Models for Hardware-Aware Neural Architecture Search. In *Proceedings of the  
1702 62nd ACM/IEEE Design Automation Conference (DAC)*. 1–6. 97.6% accuracy  
1703 surrogate model framework for HW-aware NAS.
- [54] Amir Nasr-Esfahany et al. 2025. Concorde: Fast and Accurate CPU Performance  
1704 Modeling with Compositional Analytical-ML Fusion. In *Proceedings of the 52nd  
1705 Annual International Symposium on Computer Architecture (ISCA)*. 1–15. Hybrid  
1706 analytical-ML approach achieving 2% CPI error at 5 orders of magnitude faster  
1707 than gem5.
- [55] NVIDIA Corporation. 2019. Nsight Compute: Interactive Kernel Profiler. <https://developer.nvidia.com/nsight-compute>. Industry-standard GPU kernel profiling  
1708 tool with rootline analysis.
- [56] Angshuman Parashar, Priyanka Raina, Yakun Sophia Shao, Yu-Hsin Chen,  
1709 Victor A. Ying, Anurag Muber, Rangharajan Venkatesan, Brueck Khailany,  
1710 Stephen W. Keckler, and Joel Emer. 2019. Timeloop: A Systematic Approach  
1711 to DNN Accelerator Evaluation. In *Proceedings of the IEEE International Sym-  
1712 posium on Performance Analysis of Systems and Software (ISPASS)*. 304–315.  
1713 <https://doi.org/10.1109/ISPASS.2019.00042>
- [57] Jaehyun Park, Jaewan Choi, Kwanhee Kyung, Michael Jaemin Kim, Yong Suk  
1714 Kwon, Nam Sung Kim, and Jung Ho Ahn. 2024. AttAcc! Unleashing the Power of  
1715 PIM for Batched Transformer-based Generative Model Inference. In *Proceedings  
1716 of the 29th ACM International Conference on Architectural Support for Programming  
1717 Languages and Operating Systems (ASPOLOS)*. 1–16. PIM-based accelerator for  
1718 batched transformer attention. Seoul National University/UICU.
- [58] Adam Paszke, Sam Gross, Francisco Massa, Adam Lerer, James Bradbury, Gregory  
1719 Chanhan, Trevor Killeen, Zeming Lin, Natalia Gimelshein, Luca Antiga, et al. 2019.  
PyTorch: An Imperative Style, High-Performance Deep Learning Library. In  
1720 *Advances in Neural Information Processing Systems (NeurIPS)*, Vol. 32. 8024–8035.
- [59] Pratyush Patel, Esha Choukse, Chaojie Zhang, Aakankshi Shah, Íñigo Goiri,  
1721 Saeed Maleki, and Ricardo Bianchini. 2024. Splitwise: Efficient Generative LLM  
1722 Inference Using Phase Splitting. In *Proceedings of the 51st Annual International  
1723 Symposium on Computer Architecture (ISCA)*. 118–132. <https://doi.org/10.1109/ISCA59077.2024.00019> Best Paper Award.
- [60] Hang Qi, Evan R. Sparks, and Ameet Talwalkar. 2017. Paleo: A Performance  
1724 Model for Deep Neural Networks. In *Proceedings of the 5th International Con-  
1725 ference on Learning Representations (ICLR)*. <https://openreview.net/forum?id=SyVVJ85lg>
- [61] Aurick Qiao, Sang Keun Agrawal, Anand Jayarajan, Moustafa Mittal, Amar Altaf,  
1726 Michael Cho, and Gennady Pekhimenko. 2021. Pollux: Co-adaptive Cluster  
1727 Scheduling for Goodput-Optimized Deep Learning. In *Proceedings of the 15th  
1728 USENIX Symposium on Operating Systems Design and Implementation (OSDI)*.  
1729 1–18. Goodput estimation for co-optimizing resource allocation and training  
1730 hyperparameters.
- [62] Jonathan Ragan-Kelley, Connally Barnes, Andrew Adams, Sylvain Paris, Frédéric  
1731 Durand, and Saman Amarasinghe. 2013. Halide: A Language and Compiler  
1732 for Optimizing Parallelism, Locality, and Recomputation in Image Processing  
1733 Pipelines. In *Proceedings of the 34th ACM SIGPLAN Conference on Programming  
1734 Language Design and Implementation (PLDI)*. 519–530. <https://doi.org/10.1145/2707828.2707829>

- [1741] 2491956.2462176 Pioneered separation of algorithm and schedule with learned  
1742 cost models for autoscheduling.

[63] Samyam Rajbhandari, Jeff Rasley, Olatunji Rber, and Yuxiong He. 2020. ZeRO: Memory Optimizations Toward Training Trillion Parameter Models. In *Proceedings of the International Conference on High Performance Computing, Networking, Storage and Analysis (SC)*. 1–16. <https://doi.org/10.1109/SC41405.2020.00024>

[64] Mehdi Rakhshanfar and Aliakbar Zarandi. 2021. A Survey on Machine Learning-based Design Space Exploration for Processor Architectures. *Journal of Systems Architecture* 121 (2021), 102339. <https://doi.org/10.1016/j.jsysarc.2021.102339>

[65] Saeed Rashidi, Srinivas Srinivasan, Kazem Hamedani, and Tushar Krishna. 2020. ASTRA-SIM: Enabling SW/HW Co-Design Exploration for Distributed DL Training Platforms. In *Proceedings of the IEEE International Symposium on Performance Analysis of Systems and Software (ISPASS)*. 81–92. <https://doi.org/10.1109/ISPASS48437.2020.00018>

[66] Vijay Janapa Reddi et al. 2025. MLPerf Power: Benchmarking the Energy Efficiency of Machine Learning Inference. In *Proceedings of the IEEE International Symposium on High Performance Computer Architecture (HPCA)*. 1–14. Energy efficiency benchmarking for ML inference workloads.

[67] Vijay Janapa Reddi, Christine Cheng, David Kanter, Peter Mattson, Guenther Schmuelling, Carole-Jean Wu, Brian Anderson, Maxim Breeshekov, Mark Duber, et al. 2020. MLPerf Inference Benchmark. In *Proceedings of the 47th International Symposium on Computer Architecture (ISCA)*. 446–459. <https://doi.org/10.1109/ISCA45697.2020.00045> Standard ML inference benchmark suite with server and offline scenarios.

[68] George F. Riley and Thomas R. Henderson. 2010. The ns-3 Network Simulator. *Modeling and Tools for Network Simulation* (2010), 15–34. [https://doi.org/10.1007/978-3-642-12331-3\\_2](https://doi.org/10.1007/978-3-642-12331-3_2)

[69] Arun F. Rodrigues, K. Scott Hemmert, Brian W. Barrett, Chad Kersey, Ron Oldfield, Marlo Weston, R. Risen, Jeanine Cook, Paul Rosenfeld, Elliott Cooper-Balis, and Bruce Jacob. 2012. The Structural Simulation Toolkit. In *ACM SIGMETRICS Performance Evaluation Review*, Vol. 38. 37–42. <https://doi.org/10.1145/1964218.1964225> Modular framework for system-level simulation, widely used for HPC and interconnect modeling.

[70] Ananda Samajdar, Yuhao Zhu, Paul Whatmough, Matthew Mattina, and Tushar Krishna. 2019. A Systematic Methodology for Characterizing Scalability of DNN Accelerators using SCALE-Sim. In *Proceedings of the IEEE International Symposium on Performance Analysis of Systems and Software (ISPASS)*. 58–68. <https://doi.org/10.1109/ISPASS.2019.00016> Cycle-accurate systolic array simulator for DNN accelerator DSE.

[71] Zhuomin Shen, Jaeho Kim, et al. 2025. AQUA: Network-Accelerated Memory Offloading for LLMs in Scale-Up GPU Domains. In *Proceedings of the 30th ACM International Conference on Architectural Support for Programming Languages and Operating Systems (ASPLoS)*. 1–16. <https://doi.org/10.1145/3676641.3715983> Improves LLM inference responsiveness by 20x through network-accelerated memory offloading.

[72] Mohammad Shoeybi, Mostofa Patwary, Raul Puri, Patrick LeGresley, Jared Casper, and Bryan Catanzaro. 2020. Megatron-LM: Training Multi-Billion Parameter Language Models Using Model Parallelism. In *arXiv preprint arXiv:1909.08053*. Intra-layer tensor parallelism for large language model training.

[73] Srinivas Sridharan, Taekyung Heo, Jinwoo Choi, Garyfallia Yu, Saeed Rashidi, William Won, Zhaodong Meng, and Tushar Krishna. 2023. Chakra: Advancing Performance Benchmarking and Co-design using Standardized Execution Traces. *arXiv preprint arXiv:2305.14516* (2023).

[74] Foteini Strati, Zhendong Zhang, George Manos, Ixeia Sanchez Periz, Qinghao Hu, Tiancheng Chen, Berk Buzcu, Song Han, Pamela Delgado, and Ana Klimovic. 2025. Sailor: Automating Distributed Training over Dynamic, Heterogeneous, and Geo-distributed Clusters. In *Proceedings of the 30th ACM Symposium on Operating Systems Principles (SOSP)*. 1–18. Automated distributed training with runtime/memory simulation over heterogeneous resources. ETH Zurich/MIT.. Ondrej Sykora, Alexis Rucker, Charith Mendis, Rajkishore Barik, Phitchaya Mangpo Phothilimhana, and Saman Amarasinghe. 2022. GRANITE: A Graph Neural Network Model for Basic Block Throughput Estimation. In *Proceedings of the IEEE International Symposium on Workload Characterization (IISWC)*. 1–13. <https://doi.org/10.1109/IISWC55918.2022.00014>

[76] Vivienne Sze, Yu-Hsin Chen, Tien-Ju Yang, and Joel S. Emer. 2017. Efficient Processing of Deep Neural Networks: A Tutorial and Survey. In *Proceedings of the IEEE*, Vol. 105. 2295–2329. <https://doi.org/10.1109/JPROC.2017.2761740> Canonical DNN accelerator taxonomy covering dataflows, data reuse, and energy efficiency.

[77] Philippe Tillet, H. T. Kung, and David Cox. 2019. Triton: An Intermediate Language and Compiler for Tiled Neural Network Computations. In *Proceedings of the 3rd ACM SIGPLAN International Workshop on Machine Learning and Programming Languages (MAPL)*. 10–19. <https://doi.org/10.1145/3315508.3329973> Tile-based GPU programming with heuristic performance model for kernel generation.

[78] Jan Treibig, Georg Hager, and Gerhard Wellein. 2010. LIKWID: A Lightweight Performance-Oriented Tool Suite for x86 Multicore Environments. In *Proceedings of the 39th International Conference on Parallel Processing Workshops (ICPPW)*. 207–216. <https://doi.org/10.1109/ICPPW.2010.38> Lightweight tools for thread/cache topology, affinity, and performance counter measurement.

[79] Adrian Tschan, Mohamed Awad, et al. 2025. SwizzlePerf: Hardware-Aware LLMs for GPU Kernel Performance Optimization. *arXiv preprint arXiv:2508.20258* (2025). LLM-based spatial optimization for GPU kernels, up to 2.06x speedup via swizzling.

[80] Xizheng Wang, Qingxu Li, Yichi Xu, Gang Lu, Heyang Zhou, Sen Zhang, Yikai Zhu, Yang Liu, Pengcheng Zhang, Kun Qian, et al. 2025. SimAI: Unifying Architecture Design and Performance Tuning for Large-Scale LLM Training with Scalability and Precision. In *Proceedings of the 22nd USENIX Symposium on Networked Systems Design and Implementation (NSDI)*. 1–18. Full-stack LLM training simulator achieving 98.1% alignment with real-world results. Alibaba Cloud/Tsinghua.

[81] Zixian Wang et al. 2025. SynPerf: Synthesizing High-Performance GPU Kernels via Pipeline Decomposition. *arXiv preprint* (2025). Under review.

[82] Samuel Williams, Andrew Waterman, and David Patterson. 2009. Roofline: An Insightful Visual Performance Model for Multicore Architectures. *Commun. ACM* 52, 4 (2009), 65–76. <https://doi.org/10.1145/1498765.1498785>

[83] William Won, Taekyung Heo, Saeed Rashidi, Saeed Talati, Srinivas Srinivasan, and Tushar Krishna. 2023. ASTRA-sim2.0: Modeling Hierarchical Networks and Disaggregated Systems for Large-Model Training at Scale. In *Proceedings of the IEEE International Symposium on Performance Analysis of Systems and Software (ISPASS)*. 283–294. <https://doi.org/10.1109/ISPASS57527.2023.00035>

[84] Yannan Nellie Wu, Joel Emer, and Vivienne Sze. 2022. Sparseloop: An Analytical Approach to Sparse Tensor Accelerator Modeling. In *Proceedings of the 55th IEEE/ACM International Symposium on Microarchitecture (MICRO)*. 1–15. <https://doi.org/10.1109/MICRO56248.2022.00078>

[85] Gyeong-In Yu, Joo Seong Jeong, Geon-Woo Kim, Soojeong Kim, and Byung-Gon Chun. 2022. ORCA: A Distributed Serving System for Transformer-Based Generative Models. In *Proceedings of the 16th USENIX Symposium on Operating Systems Design and Implementation (OSDI)*. 521–538.

[86] Geoffrey X. Yu, Yubo Gao, Pavel Golber, and Asaf Cidon. 2021. Habitat: A Runtime-Based Computational Performance Predictor for Deep Neural Network Training. In *Proceedings of the USENIX Annual Technical Conference (ATC)*. 503–521.

[87] Yi Zhai, Yu Cheng Wang, Peng Jiang, and Congming Kang. 2023. TLP: A Deep Learning-based Cost Model for Tensor Program Tuning. In *Proceedings of the 28th ACM International Conference on Architectural Support for Programming Languages and Operating Systems (ASPLOS)*. 833–845. <https://doi.org/10.1145/3575693.3575736>

[88] Li Lyra Zhang, Shihao Han, Jianyu Wei, Ningxin Zheng, Ting Cao, Yuqing Yang, and Yunxin Liu. 2021. nn-Meter: Towards Accurate Latency Prediction of Deep-Learning Model Inference on Diverse Edge Devices. In *Proceedings of the 19th Annual International Conference on Mobile Systems, Applications, and Services (MobiSys)*. 81–93. <https://doi.org/10.1145/3458864.3467882> Best Paper Award.

[89] Lianmin Zheng, Chengfan Jia, Minmin Sun, Zhao Wu, Cody Hao Yu, Ameer Haj-Ali, Yida Wang, Jun Yang, Danyang Zhuo, Koushik Sen, Joseph E. Gonzalez, Ion Stoica. 2020. Ansor: Generating High-Performance Tensor Programs for Deep Learning. In *Proceedings of the 14th USENIX Symposium on Operating Systems Design and Implementation (OSDI)*. 863–879.

[90] Lianmin Zheng, Ruochen Liu, Junru Shao, Tianqi Chen, Joseph E. Gonzalez, Ion Stoica, and Zhihao Zhang. 2021. TenSet: A Large-scale Program Performance Dataset for Learned Tensor Compilers. In *Advances in Neural Information Processing Systems (NeurIPS)*, Vol. 34. 29876–29888.

[91] Yinmin Zhong, Shengyu Liu, Junda Chen, Jianyu Hu, Yibo Zhu, Xuanzhe Liu, Xin Jin, and Hao Zhang. 2024. DistServe: Disaggregating Prefill and Decoding for Goodput-optimized Large Language Model Serving. In *Proceedings of the 18th USENIX Symposium on Operating Systems Design and Implementation (OSDI)*. 1–18.